THE JOURNAL OF PHYSICAL CHEMISTRY A

Feature Article

pubs.acs.org/JPCA

Organic Constituents on the Surfaces of Aerosol Particles from Southern Finland, Amazonia, and California Studied by Vibrational Sum Frequency Generation

Carlena J. Ebben,[†] Mona Shrestha,[†] Imee S. Martinez,[†] Ashley L. Corrigan,[‡] Amanda A. Frossard,[‡] Wei W. Song,[§] David R. Worton,[∥,⊥] Tuukka Petäjä,[#] Jonathan Williams,[§] Lynn M. Russell,[‡] Markku Kulmala,[#] Allen H. Goldstein,[∥,▽] Paulo Artaxo,[○] Scot T. Martin,[◆] Regan J. Thomson,[†] and Franz M. Geiger*[,†]

[†]Department of Chemistry, Northwestern University, 2145 Sheridan Road, Evanston, Illinois 60208, United States

[‡]Scripps Institution of Oceanography, University of California, San Diego, La Jolla, California 92093, United States

[§]Max Planck Institute for Chemistry, 55128 Mainz, Germany

[∥]Department of Environmental Science, Policy and Management, University of California, Berkeley, California 94720, United States

[⊥]Aerosol Dynamics, Inc., Berkeley, California 94710, United States

[#]Department of Physics, FI-00014 University of Helsinki, Finland

[▽]Department of Civil and Environmental Engineering, University of California, Berkeley, California 94720, United States

[○]Institute of Physics, University of São Paolo, Rua do Matão, Travessa R, 187, 05508-090, São Paolo, Brazil

[◆]School of Engineering and Applied Sciences & Department of Earth and Planetary Sciences, Harvard University, 29 Oxford Street, Cambridge, Massachusetts 02138, United States

ABSTRACT: This article summarizes and compares the analysis of the surfaces of natural aerosol particles from three different forest environments by vibrational sum frequency generation. The experiments were carried out directly on filter and impactor substrates, without the need for sample preconcentration, manipulation, or destruction. We discuss the important first steps leading to secondary organic aerosol (SOA) particle nucleation and growth from terpene oxidation by showing that, as viewed by coherent vibrational spectroscopy, the chemical composition of the surface region of aerosol particles having sizes of 1 μm and lower appears to be close to size-invariant. We also discuss the concept of molecular chirality as a chemical marker that could be useful for quantifying how chemical constituents in the SOA gas phase and the SOA particle phase are related in time. Finally, we describe how the combination of multiple disciplines, such as aerosol science, advanced vibrational spectroscopy, meteorology, and chemistry can be highly informative when studying particles collected during atmospheric chemistry field campaigns, such as those carried out during HUMPPA-COPEC-2010, AMAZE-08, or BEARPEX-2009, and when they are compared to results from synthetic model systems such as particles from the Harvard Environmental Chamber (HEC). Discussions regarding the future of SOA chemical analysis approaches are given in the context of providing a path toward detailed spectroscopic assignments of SOA particle precursors and constituents and to fast-forward, in terms of mechanistic studies, through the SOA particle formation process.

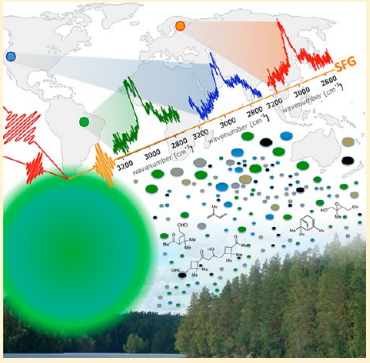

I. MOTIVATION AND CHALLENGES

The 2007 IPCC Report states that the role of aerosols in the climate system "*remains the dominant uncertainty in radiative forcing.*"[1] Despite this prominent role, the level of scientific understanding regarding aerosols has been rated "very low" for close to a decade,[1,2] contributing significantly to the large (>50%) uncertainty associated with the net anthropogenic radiative forcing estimates that range from +0.6 to 2.4 W m^{-2}. Of particular importance are secondary organic aerosol (SOA) particles, whose formation can be associated with the emission of biogenic volatile organic compounds (BVOCs) from the Earth's large forest ecosystems, some of which range from continental to global spatial scales (Figure 1A). Boreal forests, for instance, span more than twelve time zones of the Northern Hemisphere, whereas the tropical forests encompass somewhat more than one-third of the equator. To provide a scale of the impact that SOA particles formed from BVOCs emitted from forests can have on the climate system, we point out that SOA production over the Finnish boreal forest results in up to −14 W m^{-2} radiative forcing, compared to a global mean of up to −1.1 W m^{-2}.[3]

Received: March 19, 2012
Revised: June 4, 2012
Published: June 26, 2012

   dx.doi.org/10.1021/jp302631z | *J. Phys. Chem. A* 2012, 116, 8271−8290

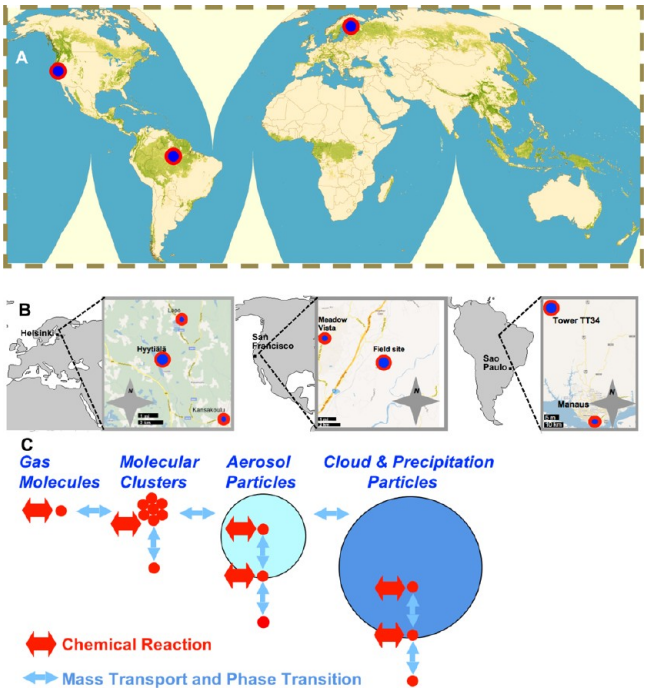

Figure 1. Global map of the canopy height of the Earth's forests, with dark green indicating heights of up to 70 m, and field sampling locations indicated (A). Figure 1A is adapted from http://www.nasa.gov/images/content/470377main_globaltreecanopy_cutoutmap.jpg. European field sampling location at Hyytiälä, Finland, North American field sampling location at Blodgett Forest, and South American field sampling site at Tower TT34 in the central Amazon Basin (B). (C) Aerosol particle formation mechanisms involving gas phase species, molecular clusters, aerosol particles, and cloud and precipitation particles undergoing interfacial processes, chemical reactions (thick red arrows), mass transport (thin light blue arrows), and phase transitions (filled red, light blue, and dark blue circles). Adapted from Pöschl et al.[202]

The strong positive temperature dependence of BVOC emissions[4−6] could possibly increase the importance of SOA particles for future, warmer climates,[7] provided that higher BVOC concentrations coincide with higher SOA particle concentrations. Many important climate-related chemical and physical processes involving SOA particles occur at their surfaces, yet as we will show below, it is exceedingly difficult to study the interfacial region between the aerosol gas phase and the aerosol particle phase directly.

In this Feature Article, we relate how we connected with established field and laboratory projects studying SOA particles, how we applied coherent vibrational spectroscopy to study the surfaces of SOA particles, and what we learned from our spectroscopic studies in terms of SOA particle formation. This work addresses several critical needs in aerosol analytics and the chemical composition of the species that are involved in SOA particle formation. Specifically, we believe that physical chemists are confronted with the following five research challenges:

(i) Though vitally needed for improving computer modeling efforts aimed at quantitatively predicting SOA particle yields for a given atmospheric gas phase composition,[8] the molecularity of even the first few reactions leading to SOA particle formation is not known and thus needs to be determined;

(ii) Although the SOA particle surface region connects the aerosol particle phase with the aerosol gas phase, little molecular-level information is available about it;

(iii) Specific chemical markers need to be developed for quantifying how chemical constituents in the SOA gas phase and the SOA particle phase are related in time;

(iv) Nondestructive methods applicable at ambient pressure and temperature need to be developed for the chemical analysis of SOA particles; and

(v) The expertise for SOA particle sampling is typically not found in chemistry departments but rather in atmospheric science and chemical engineering departments, requiring students to master multiple disciplines.

To address these challenges and show one way of how they may be overcome, we summarize and compare our results from the application of coherent vibrational spectroscopy, specifically vibrational sum frequency generation (SFG), to the surfaces of aerosol particles collected in the central Amazon Basin,[9] chosen as an example of a tropical forest, in Southern Finland,[3] chosen as an example of the boreal forest, and in Blodgett Forest, California,[10] an anthropogenically influenced ponderosa pine forest (Figure 1B). Tropical forest air is typically rich in isoprene, whereas air over the boreal and the pine forests is typically rich in α-pinene, and we expect the vibrational spectra obtained from the particles to be due to oxidation products of these compounds in the particle phase. By working with the Harvard Environmental Chamber (HEC),[11] we compare the results from the natural samples with those obtained from synthetic model systems. We learn from our studies that in addition to its surface selectivity, SFG spectroscopy can provide a substantial sensitivity advantage over other nondestructive methods that can be performed under ambient temperature and pressure conditions, and that SFG is most informative when it is combined with the full range of aerosol particle and gas phase analytics that are typical of large-scale atmospheric chemistry field campaigns such as AMAZE-08,[9] HUMPPA-COPEC-2010,[3] or BEARPEX-2009.[12]

II. ORGANIZATION

Prior to describing our findings and discussing the results, we provide here an overview of the organization of this Feature Article. We begin by summarizing the current state of knowledge regarding the chemical mechanisms for SOA particle formation in section III. Section IV contains the description of the three field measurement sites where the particles studied here were collected. Sections V and VI continue with a discussion of the standard methods for aerosol particle collection, synthesis, sizing, and chemical analysis. As the particle collection methods available at the field sampling sites were not identical, the purpose of the section on particle collection and analytics (sections V and VI) is to provide details of the instrumentation. Section VI also contains a section on aerosol particle synthesis for laboratory modeling studies that can be used to interpret results obtained from the field-derived particles. Section VII provides an overview of the coherent vibrational spectroscopy used to analyze the aerosol particle phase, and section VIII provides results regarding synthetic modeling studies carried out at the HEC. The results from the field-derived particles are discussed in sections IX−XI, and section XII summarizes this work.

III. SOA PARTICLE FORMATION

From a chemist's perspective, the low level of scientific understanding regarding the impact of aerosol particles in the

dx.doi.org/10.1021/jp302631z | J. Phys. Chem. A 2012, 116, 8271−8290

Table 1. Range of Concentrations of Temperature, Relative Humidity, OH, O_3, various Monoterpenes, and O/C Ratio Relevant in Southern Finland, the Central Amazon Basin, and Northern California for the Particle Sampling Periods Relevant for This Work

species	southern Finland[a]	central Amazon[b]	northern California[c]
temp (°C)	25 (night) to 32 (day)	22 (night) to 32 (day)	8 (night) to 32 (day)
RH (%)	30−60 (night) to 80−100 (day)	60 (night) to 100 (day)	20−30 (night) to 50−70 (day)
OH (10^6 cm^{-3})	0.2−3.0	1−3[d] and 5[e]	0.04−14.67
NO (ppb)	0.1	0.1	0.04−0.17[f]
O_3 (ppb)	20−70	1−20	9.7−98.7
isoprene (ppb)	0.01−0.70	1−9	0.33−5.79[g]
α-pinene (ppb)	0.01−1.0	0.01−0.40	0.11−0.61[g]
β-pinene (ppb)	0.01−0.20	0.008−0.080	0.07−0.35[g]
limonene (ppb)	n.a.	0.008−0.080[d]	n.a.
O/C ratio	0.5−0.7	0.4 +/ −0.1[h]	0.4−0.9

[a]Please see Williams et al. for details.[3] [b]Please see Martin et al. for details.[9] [c]Please see Worton et al. for details.[10] [d]Data from Karl et al.[203] for the same location at which AMAZE-08 took place. [e]Data for the tropical forest boundary layer from Lelieveld et al.[204] [f]Personal communication with R. C. Cohen and E. C. Browne. NO data for 10AM through 6PM; all other data for day and night. [g]Data from G. Schade. [h]Please see Chen et al.[11]

climate system is rooted largely in a lack of molecular level information regarding

(i) the formation of aerosols,
(ii) their surface properties,
(iii) their chemical composition and physical properties, and
(iv) the reactions that take place in the multiphase environment that is emblematic of aerosol chemistry (Figure 1C).[13,14]

Similar to the case of the early research on stratospheric ozone depletion,[15] the lack of molecular information regarding these key processes has led to the situation where mismatches between atmospheric field measurements and computer simulations are often attributed to unknown chemistry. As a result, the processes that drive much of the chemistry in the climate system are the focus of intense, often multi-investigator chemical research programs.[13,16−33] SOA particle formation in particular ranks among the least understood atmospheric processes in the climate system.[8,34−37] Yet, substantial advances have been made recently in terms of molecular studies linking BVOC emissions to the aerosol particle phase:[38−41] relevant reaction pathways have been identified that begin with oxidation, such as ozonolysis of a C=C double bond.[42−44] In the case of the ozonolysis of α-pinene, which is a monoterpene typically observed in highest concentrations in boreal forests, this oxidation process leads to the formation of less-volatile organic compounds, such as pinonaldehyde and pinonic acid. Dimerization and oligomerization processes have been reported to be important as well,[45−48] along with the formation of pinic acid and terpenylic acid.[49] Likewise, the oxidation of isoprene, which is the dominant plant emission in tropical forests, has been reported to involve species such as epoxides, which also exhibit lower volatility and higher solubility than isoprene in aerosol and/or cloud droplets.[50,51] The lower vapor pressures of the oxidized compounds[52−55] can lead to their condensation, ultimately contributing, along with aqueous phase pathways, to the production and growth of SOA particles.[45−48]

Many of the implicated reactions involve condensations between the various reactive and stable species that are produced from the photochemical oxidation and ozonolysis of C=C double bonds present within biogenic terpenes. For instance, Kroll and Seinfeld[53] proposed that the formation of peroxyhemiacetals, hemiacetals, sulfate esters, adducts of stable Criegee intermediates, anhydrides, and aldol products may occur under tropospheric conditions; however, the mechanisms of these proposed reaction pathways have not yet been tested in a systematic fashion. This is in part due to the difficulty in carrying out the chemical analysis of SOA particles, especially if one wishes to study them with nondestructive methods that are applicable under ambient pressure and temperature conditions. Here, we show one way how to solve this issue. We begin our discussion by reviewing the aerosol particle sampling locations.

IV. AEROSOL PARTICLE SAMPLING LOCATIONS

The boreal forest field site we worked at during the summer of 2010[3] is located at the Station for Measuring Forest Ecosystem-Atmosphere Relations (SMEAR II)[56] at Hyytiälä (61°51′ N, 24°17′ E) in Southern Finland (Figure 1B, left panel). The site is 230 km north of Helsinki, 170 m above sea level, and surrounded by boreal forest. The predominant tree species is scots pine (*Pinus sylvestris*) with some spruce (*Picea abies*), aspen (*Populus species*), and birch (*Betula species*). Anthropogenic influences at the site are generally low, particularly when the wind comes from the sparsely populated northern sector. Transport of aged particulate matter also occurred from urban areas upwind. During the 2010 field intensive, the site rarely received wind from the NW/NE but instead often experienced SW flow from industrialized Europe, especially during the second half of the campaign. Incidental pollution from forest management activities and minor traffic did occur during the field intensive and was readily identified by aromatic compounds such as toluene and benzene in the gas phase. A 72 m tall tower was used for measurements of meteorological, physical, and chemical parameters at various heights above the 16 m canopy top (please see Williams et al.[3] for further details). The relevant meteorological conditions for the site are listed in Table 1.

The tropical forest field site is located at tower TT34,[9] which is situated within a pristine terra firme rainforest in the Reserva Biologica do Cuieiras and managed by the Instituto Nacional de Pesquisas da Amazonia (INPA) and the Large-Scale Biosphere-Atmosphere Experiment in Amazonia (LBA), 60 km NNW of downtown Manaus (Figure 1B, right panel). The forest canopy height near the tower varies between 30 and 35 m; the sampling height on the tower is 38.75 m. Andreae et al.[57] summarized meteorological and climatological information typical of the climatology at the reserve. Relevant data for AMAZE-08 are summarized in Table 1. Briefly, VOC emissions in the Amazon Basin are the Earth's largest[58−60] and far outweigh anthropogenic emissions. Along with a high solar flux, there is a large source of OH radicals in the gas phase,[61] which dominates SOA production chemistry. In contrast, SOA production due to reactions involving ozone is less important due to relatively low ozone

dx.doi.org/10.1021/jp302631z | J. Phys. Chem. A 2012, 116, 8271−8290

concentrations (5−20 ppb). Overall, the central Amazon represents a pristine environment that is characterized by having nearly pure biogenic aerosol particles during the wet season (October through March).[62−67] Specifically, up to 90% of the atmospheric particles sampled in the fine mode (size less than 1 μm) were composed of SOA particles formed by atmospheric oxidation and gas-to-particle conversion of BVOCs.[68] This characteristic makes the area an ideal natural laboratory to isolate natural SOA production and thereby provide a baseline understanding against which to measure anthropogenic influences.

Finally, we also studied particles collected during the Biosphere Effects on AeRosols and Photochemistry EXperiment (BEARPEX)[10,12,69] 2009 Campaign in Blodgett Forest, which is a ponderosa pine (*Pinus ponderosa*) forest, located in the foothills of the Sierra Nevada Mountains of Northern California (38° 59′ N, 120° 58′ W, Figure 1B, center panel) at an elevation of 1315 m. The forest canopy height in 2009 was approximately 8 m and the sampling height on the tower was 9.3 m. This site has a Mediterranean climate, with very little precipitation during the summer months. The typical daytime air mass trajectory is upslope flow from the southwest, from the populated Sacramento Valley, and transects a 30 km band of oak trees approximately half way between Sacramento and the site. In general, one finds that isoprene concentrations are higher than α-pinene at Blodgett Forest in the afternoon, even though they have been substantially processed during transport to the site. α-Pinene concentrations are higher than isoprene in the morning and evening as a result of temperature driven local emissions into a shallow boundary layer. At night the most common trajectory is downslope flow from the Sierra Nevada Mountains northeast of the site.[12,69,70] As a result of strong orographic forcing, the daily wind speed and direction patterns are nearly constant year round. Every afternoon the urban plume from Sacramento impacts the site, bringing with it substantial oxidized isoprene emissions from a 30 km wide band of oak trees located in the foothills several hours upwind, and the potential for significant anthropogenic influence in the formation of secondary organic particle material. Some of the relevant conditions are summarized in Table 1.

V. COLLECTION OF AEROSOL PARTICLES

In general, the collection of aerosol particles is carried out such that various size ranges are sampled to evaluate particles in the fine (<1 μm) and coarse (>1 μm) modes. Particulate matter with sizes below 1 μm (PM1) or 2.5 μm (PM2.5) can be collected selectively by using a cyclone, used in this work for the collection of aerosol particles in Finland (PM1) and in California (PM2.5). An example of such a PM1 particle sampler is shown in Figure 2A. More sophisticated approaches employ the use of micro-orifice uniform-deposit impactors (MOUDI, Figure 2B),[71] which can yield highly size-resolved particle samples down to ten nanometers, depending on the model. Such an approach was used in this work for the collection of particles in the central Amazon Basin. Particle sizing within a MOUDI is subject to log-normal size distributions, and when several sizes are collected simultaneously on several stages, some spillover of larger particles onto a stage sampling particles with smaller sizes can occur. Sampling methods using a cyclone or a MOUDI result in low particle loadings unless long collection times are employed, typically corresponding to a mass of a few micrograms or less on a given filter or stage, which are distributed over a 37 mm or 47 mm surface for the studies presented here. Therefore, the analysis of aerosol particles collected in such a fashion represents a classical "detection limit" problem for some situations and curtails the analysis of particles collected over short times or while their concentrations in the air at the time of collection are low.

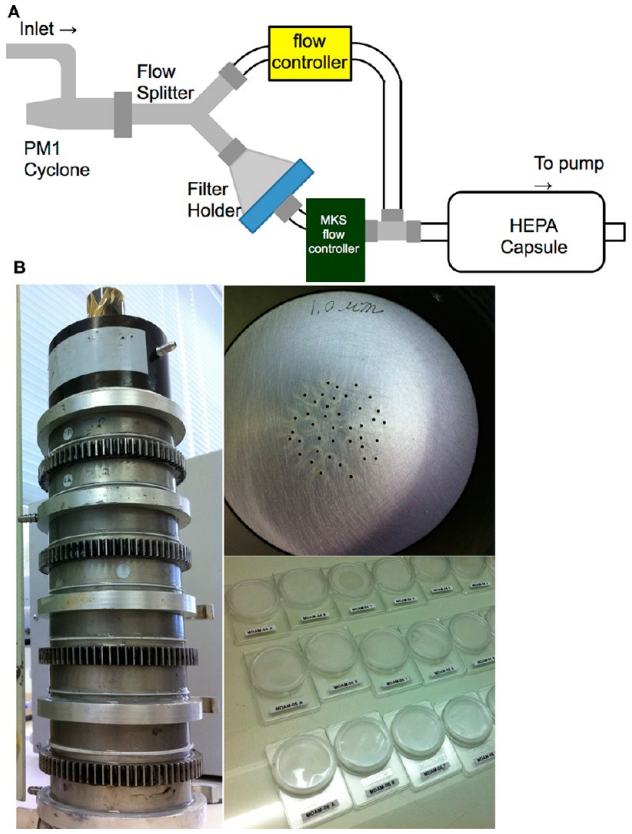

Figure 2. (A) Home-built particle sampler for collecting particles having aerodynamic diameters below 1 μm used at Northwestern University consisting of a PM1 cyclone (URG Corporation, part no. URG-2000-30EHB), which size-selects submicrometer particles, connected to a flow splitter (Brechtel Manufacturing Inc., model 1102) and operating such that a gas flow of approximately 5.1 slpm is directed through a 47 mm closed aluminum filter holder (BGI Incorporated, part no. F1) whereas approximately 11.6 slpm pass through a bypass line. A HEPA capsule is placed before a vacuum pump, which pulls flow through the system. Particles are collected on Teflon filters (Pall Life Sciences, 47 mm diameter, 1 μm pore size, part no. 28139-125) and kept in a freezer until analysis. (B) Micro-orifice uniform-deposit impactor (MOUDI) used in the Amazon Basin showing the (left) first four stages of size separation, the multiple nozzles for the 1.0 μm stage (top right), a subset of the MOUDI impactor substrates sampled for this work in the central Amazon Basin (bottom right).

VI. AEROSOL PARTICLE ANALYTICS

To fully understand the role that secondary organic aerosol particles play in our climate system, several properties of the particles are needed, including size and chemical composition. A wide range of analytical tools have been developed and repeatedly improved upon to determine these properties. Use of a combination of these tools is nearly always the best way to obtain a cohesive picture of SOA properties.

A. Particle Sizing. One of the most sought-after physical properties of aerosol particles is their size distribution and its link to the direct and indirect effect of radiative forcing.[72] In this work, we heavily rely on sizing down to 3 nm in the discussion of the Finnish particle samples, including those collected during particle nucleation events. One of the most common methods

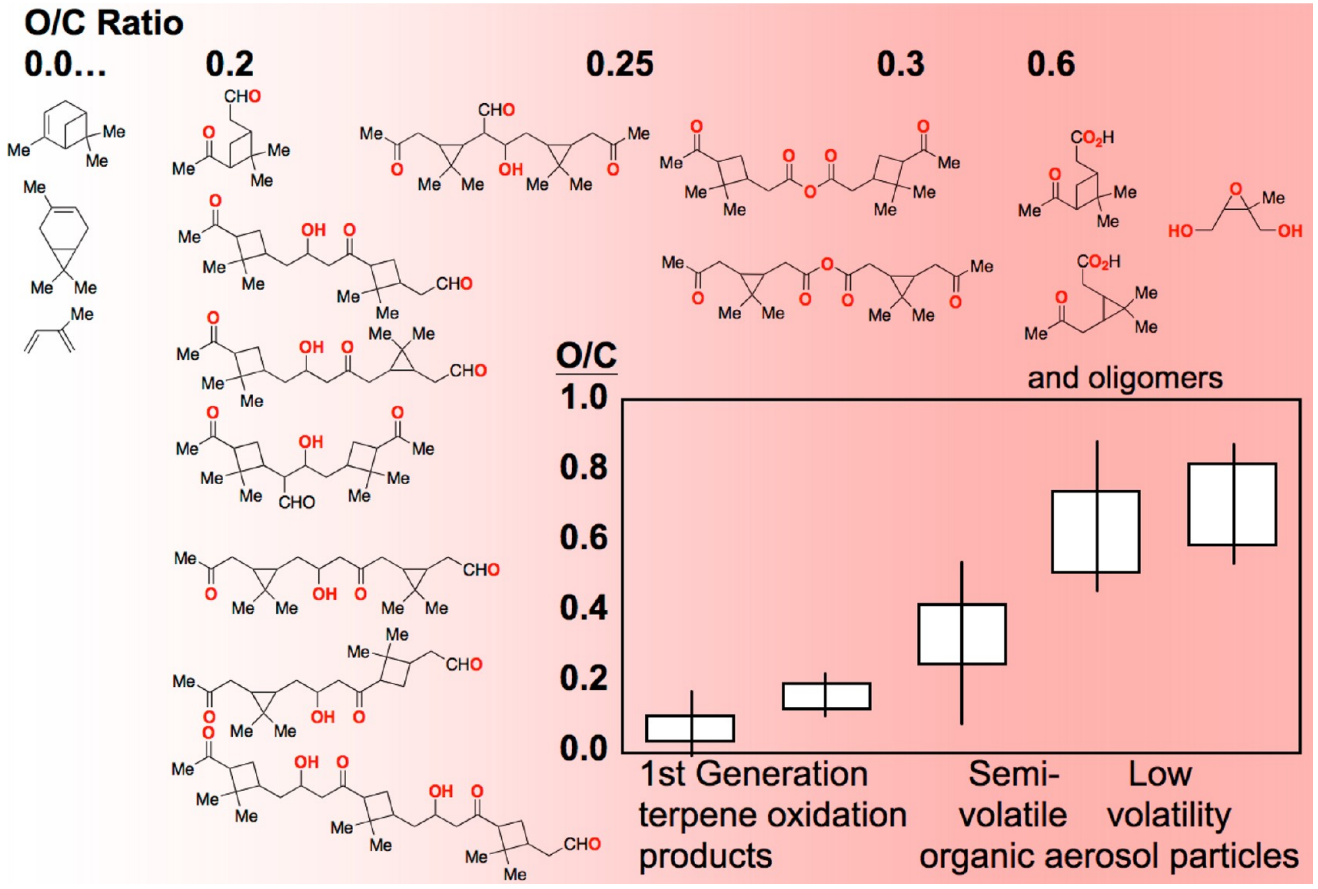

Figure 3. Selection of putative organic molecules thought to be present in secondary organic aerosol particles and corresponding oxygen-to-carbon (O/C) ratio values determined from field intensives in North and South America and Europe, adapted from Jimenez et al.[88] Vertical lines indicate uncertainties.

is a scanning mobility particle sizer (SMPS),[73] which scans through a range of voltages in a differential mobility analyzer (DMA) to quickly obtain a full particle size distribution. Multiple charging on particles and nonspherical particle shapes may lead to some inaccuracies in sizing. Concentrations of the smallest, 3 nm sized particles discussed in this work as part of the nucleation event observed in Finland on 23 July 2011 are inferred on the basis of the flux of new particles into the measurable size range, rather than being measured directly. Issues with the variety of instruments used for particle sizing include differences in the parameters used to determine particle size between techniques, as well as differences in resolution and accuracy of measurements.[74] Emerging mass spectrometric techniques approach the crucial cluster size (1−3 nm) from below. In particular, the Atmospheric Pressure interface time-of-flight mass spectrometer (APi-TOF)[75,76] can provide chemical information at high mass resolution for naturally charged ions and clusters, both in the field and in laboratory experiments, but we do not use it in this work.[77−81]

B. Chemical Composition of Secondary Organic Aerosol Particles. *1. Online Analysis.* Much of the chemical analysis of natural and synthetic SOA particles to date has been carried out using mass spectrometry.[21,82−85] The aerosol mass spectrometer (AMS)[86] has been the workhorse in the field, and high-resolution time-of-flight mass spectrometry (HR-ToF-MS) has in recent years been the preferred laboratory approach.[87,88] Benefits of mass spectrometry include the ability to assess the size and chemical composition of single particles in real time, diminishing the possibilities of artifacts or loss of volatile species that can be problems in offline analysis. The interpretation of mass spectra obtained from natural or synthetic SOA particles is based on data obtained from highly complex mixtures, which has made the process of deconvoluting the underlying molecular structures of the particle constituents challenging. For instance, the Johnston group attributed MS fragmentation patterns from SOA particles that might be derived from α-pinene aldol adducts,[89,90] but confirmation of these assignments has yet to occur. Little direct evidence for chemical structures is available, mainly because reference compounds for benchmarking and chemical identification do not exist. An important collection of data that are available, however, is the oxygen-to-carbon (O/C) ratio of various SOA particles.[88] The O/C ratios report on the oxidation state of the aerosol particle constituents, and they have been used to determine the sources of these constituents. Figure 3 summarizes the O/C ratios for a number of putative organic SOA particle constituents, along with the structures of some of these molecules and how they may relate to the SOA particle formation process. O/C ratios often provide insight into the age of particles, because the O/C ratio of a particle typically increases as it becomes more processed.[91] By working with major field campaigns, we recently reported that SOA particles from air rich in α-pinene, such as those from Southern Finland, have O/C ratios between 0.5 and 0.7,[92] whereas isoprene-rich samples from the central Amazon Basin have O/C ratios between 0.3 and 0.5.[11] Aerosol particles from Blodgett Forest are associated with an O/C ratio between 0.4 and 0.9. Other complex field-obtained mixtures of various forms

dx.doi.org/10.1021/jp302631z | J. Phys. Chem. A 2012, 116, 8271−8290

of organic aerosol particles can have O/C ratios as low as below 0.1 and as high as 0.9 (Table 1).[88]

Particles synthesized in a laboratory under controlled conditions are often used to benchmark results obtained from more chemically complex particles collected during field studies, and we take that approach here as well. Particle synthesis may take place in a flow tube or a cloud chamber, and the particles are generally evaluated by mass spectrometry, sizing techniques, and other online analyses, as well as offline techniques. The major difference between flow tube and chamber approaches is in the concentration of oxidant and precursor used to synthesize the particles. Specifically, though chamber experiments, such as those carried out at the HEC discussed here, take far longer to complete, the oxidant and monoterpene concentrations utilized are generally closer in relevance to atmospheric conditions than those employed in flow tube studies. Looking at, for example, the ozonolysis of monoterpenes in a chamber, ozone concentrations typically fall in the range of 50 ppb to 1 ppm, whereas typical monoterpene concentrations are 1−300 ppb.[93−102] Table 1 shows that atmospherically relevant conditions for the sites discussed here are on the lower end of the conditions that are possible in a typical chamber study. At the HEC, OH concentrations are approximately 7×10^6 OH radicals cm^{-3},[11] ozone concentrations used in the studies presented here are as low as 76 ppb,[92] and α-pinene and isoprene concentrations are held at around 20 and 200 ppb, respectively.[92] Even though we do not use flow tube approaches in the work presented here, we note that such experiments are highly beneficial[55,89,103−107] in that they may be completed quickly, thus allowing for the fast screening of reaction conditions and resultant aerosol particle properties to hone in on conditions for the more time-intensive chamber studies.

2. Off-line Analysis. Off-line measurements fill important gaps in the characterization of SOA particles. Ziemann and co-workers have had much success using temperature-programmed thermal desorption (TD) to obtain mass spectra of particles from chamber studies with high sensitivity, speed, and minimal sample handling.[108,109] Compounds with similar volatilities are difficult to characterize using this method; however, separation of these compounds by the use of TD-gas chromatography/mass spectrometry overcomes this limitation.[110] Another method that has been utilized in determining SOA composition is high resolution electrospray ionization mass spectrometry (HR-ESI-MS), which has been used to investigate limonene oxidation products from chamber studies following various extraction methods.[111,112] High resolution desorption electrospray ionization mass spectrometry (DESI-MS)[113] allows for less time for reactions between the solvent and particle components and features a reduced chance of breakdown of labile particle components, enabling photochemical studies associated with light-absorbing brown carbon.[114]

A shortcoming of these methods is that the particles are destroyed during analysis and are sometimes dissolved prior to destruction. Nondestructive methods for analyzing the chemical composition of SOA particles exist as well, but these methods generally involve offline analysis. In particular, cross-polarization with magic-angle spinning (CPMAS) ^{13}C NMR has been used to determine the distribution of organic functional groups within particles.[115] CPMAS ^{13}C NMR does not require dissolution of the aerosol particles in a solvent. However, this analysis requires a large amount of sample, greatly reducing temporal resolution during sample collection, as well as some sample manipulation, including separation of organic and inorganic components. Fourier transform infrared (FTIR) spectroscopy is another important tool for studying organic aerosol particles without the necessity of working under vacuum conditions, as is needed for synchrotron-based spectromicroscopy.[116] In particular, the Russell group[117] has applied transmission FTIR spectroscopy to microgram amounts of aerosol particle material on 37 mm stretched Teflon filters, allowing for an exquisite speciation analysis and source apportionment of the organic and inorganic constituents within the organic particulate matter. The ability to distinguish between organic functional groups provides increased chemical specificity versus the analysis of O/C ratios alone.[117] Also, due to the limited sensitivity of FTIR spectroscopy, particle samples are collected over longer periods of time when compared to AMS sampling times, somewhat restricting the time-resolution of speciation information. In our present work in Finland and California, particles were sampled for between 6 and 24 h and up to 3 days, respectively. The particles are dried as they are collected to prevent interference from water absorption during analysis, and the drying process may impact the chemistry of the particles, including those studied in this work by SFG spectroscopy. For both FTIR and NMR spectroscopy, quantitative analysis may be difficult, and data interpretation is often not trivial.

Other methods applied to the analysis of organic aerosol particles, which are important for the work discussed here, include electron microscopy,[118,119] as well as optical[120] and X-ray imaging.[121] The use of scanning electron microscopy (SEM) and tunneling electron microscopy (TEM) is valuable for determining the elemental composition of single particles, especially of inorganic components but are less useful in determining the oxidation states and hybridization of carbon, oxygen, and nitrogen. The use of SEM and TEM in combination with X-ray techniques provides a more complete molecular understanding of organic species. Near edge X-ray absorption fine structure (NEXAFS) and scanning transmission X-ray microscope (STXM) spectrometry have proven useful for quantifying the organic functional groups present in aerosol particle samples. The use of microscopic techniques is beneficial in that it allows for the determination of single particle chemical composition,[122] as well as morphology[123,124] with good spatial resolution. However, obtaining statistically significant results from single particle analyses can be extremely time-consuming. Currently, it is difficult to determine the chemical composition of single particles smaller than approximately 200 nm under ambient conditions and in real time.[125] As discussed in the following section, coherent laser spectroscopies can overcome some of the limitations of the techniques used for the analysis of organic aerosol particles as they are applied directly to particles collected on filters and impactors without the need for vacuum conditions, particle extraction, destruction, or other sample manipulation.

VII. VIBRATIONAL SUM FREQUENCY GENERATION (SFG) SPECTROSCOPY OF ORGANIC AEROSOL PARTICLES

SFG spectroscopy[126,127] is a powerful spectroscopic technique that has enabled much molecular insight into the heterogeneous atmospheric chemistry of laboratory model systems. The SFG signal intensity, I_{SFG}, is directly proportional to the square modulus of $\chi^{(2)}$, the second-order susceptibility of the system under investigation, and the intensity of the incident visible and

IR electric fields that are used to produce the SFG signal, I_{Vis} and I_{IR}, respectively:[128]

$$I_{SFG} \propto |\chi^{(2)}|^2 I_{Vis} I_{IR} \quad (1)$$

The second-order susceptibility consists of a nonresonant and a resonant contribution, $\chi^{(2)}_{NR}$ and $\chi^{(2)}_{R\nu}$, respectively:[128]

$$I_{SFG} \propto |\chi^{(2)}_{NR} + \sum_{\nu=1}^{n} \chi^{(2)}_{R\nu} \cdot e^{i\gamma_\nu}|^2 \quad (2)$$

In general, the nonresonant contributions to the SFG signal are small for hydrocarbons on dielectric surfaces.[129] The resonant contribution contains vibrational resonances from each oscillator at frequency ν, with n vibrational modes being coupled by their relative phases, γ_ν, and the entity is proportional to number of molecules, N_{ads}, and the molecular hyperpolarizability, β_ν, averaged over all molecular orientations at the surface:[130]

$$\chi^{(2)}_{R\nu} \propto N_{ads} \langle \beta_\nu \rangle \quad (3)$$

The molecular hyperpolarizability increases in value at resonance, i.e., when the frequency of the incoming IR beam matches a vibrational transition of the adsorbate or interface:[131]

$$\beta_\nu = \frac{A_{\nu,ij} M_{\nu,k}}{\omega_{IR} - \omega_\nu + i\Gamma_\nu} \quad (4)$$

Here, A_ν is the Raman transition probability for a given mode, M_ν is the infrared transition dipole moment of the same mode, i, j, k refer to the surface coordinate system, ω_ν is the frequency of the oscillator, ω_{IR} is the frequency of the infrared light, and Γ_ν is the damping coefficient that can be used to describe the natural line width of the oscillator. Equation 4 shows that modes observable by SFG have to be IR and Raman active.

The Geiger group has focused on oxidative C=C double bond cleavage chemistry involving flat surfaces of oxides functionalized with atmospherically relevant molecules via silane chemistry,[132−138] whereas other research groups have focused on the flat surfaces and interfaces of water.[24,26,139−146] Excellent resources outlining the details of vibrational SFG exist,[147] and some of its applications in areas ranging from biophysics[148] to catalysis[149] and energy science[150] to environmental chemistry[151] have been reported. SFG spectroscopy boasts an exquisite sensitivity to molecular structure within complex environments, a very high selectivity for environments where centrosymmetry is broken, and the possibility of heterodyne detection of weak vibrational responses, which allows for the analysis of nano-[92] to sub-femtogram[152] amounts of samples, including aerosol particles, or of samples having oscillators with weak Raman and IR transition dipole moments that are located in environments were centrosymmetry is not strongly broken. Although nonlinear optics had been applied to nano- and microparticles before,[153−158] the application of SFG to study atmospheric aerosol particles had not been presented prior to 2011, when our first reports on the subject appeared.[92,159,160] Some considerations regarding SFG signal generation from organic aerosol particles in the micrometer and submicrometer range are given in section IXA.

In the experiments (Figure 4),[135,136,138,161,162] we use a broadband 120 fs infrared optical parametric amplifier running at a 1 kHz repetition rate. SFG spectra are obtained with a hybrid scanning/broadband method pioneered by Walker and coworkers[163] by upconverting the IR light field using a visible pump beam from a regeneratively pumped Ti:S amplifier laser system filtered with a narrow-band-pass filter yielding an 800 nm pump

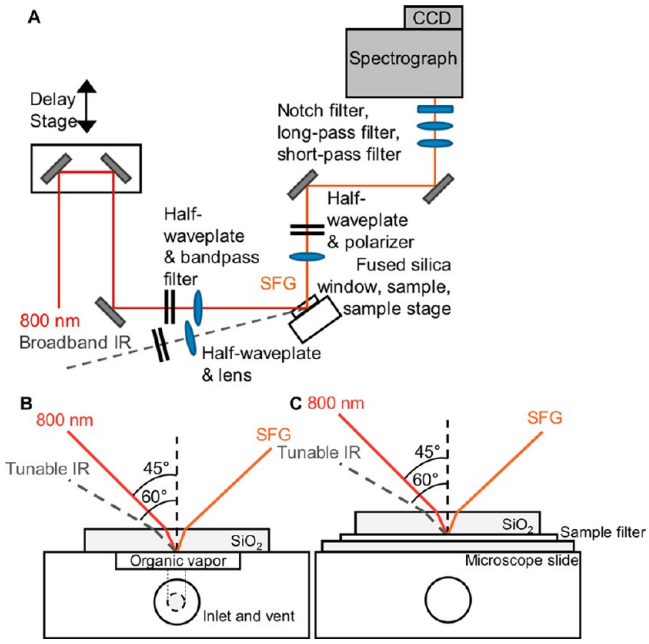

Figure 4. (A) Experimental setup used in the vibrational SFG experiments for studying (B) vapor/fused silica and (C) filter sample/fused silica interfaces. Reproduced with permission from the European Geosciences Union.

pulse with 1.57 nm bandwidth. To avoid optical damage, the incident pulse energies and foci are limited to 1 μJ and 50 μm in diameter, respectively. We reference the SFG spectra to the SFG response from a gold substrate to account for the energy distribution in the IR field for each polarization combination, normalize to input power, and calibrate to the methyl CH stretches of a spectroscopic standard composed of polystyrene.

SFG experiments probing reference compounds, all of which have sufficiently high enough vapor pressures at room temperature,[164] at the surfaces of optical windows using a previously described[165] custom-built chamber containing optical IR grade windows clamped upon a Teflon cell holding microliter amounts of liquid sample with a void space to fill it with the equilibrium vapor pressure of the sample. Prior to use, all sample cell materials are rinsed and sonicated in methanol and Millipore water, followed by nitrogen and oven drying, and then plasma cleaning. SFG spectra of the optical windows after this procedure are void of CH stretching contributions.

VIII. α-PINENE-DERIVED AEROSOL PARTICLES PREPARED AT THE HARVARD ENVIRONMENTAL CHAMBER (HEC)

Figure 5A shows ssp-polarized SFG spectra of organic aerosol particles having a size of roughly 100 nm that were collected at the HEC in 2010 and of α-pinene vapor in contact with a fused silica window.[92] We recently described the details of this experiment, including the particle synthesis and characterization.[92,159] The ssp polarization combination utilizes upconverter and infrared light that is plane-polarized parallel and perpendicular to the surface, respectively, and detects SFG signals that are polarized perpendicularly to the surface. For molecular adsorbates located at macroscopically flat substrates, such as the α-pinene reference compound adsorbed to a fused silica window (Figure 5A), the ssp polarization combination probes the components of vibrational modes that are oriented perpendicular to the surfaces. The ssp-polarized SFG spectrum

dx.doi.org/10.1021/jp302631z | J. Phys. Chem. A 2012, 116, 8271−8290

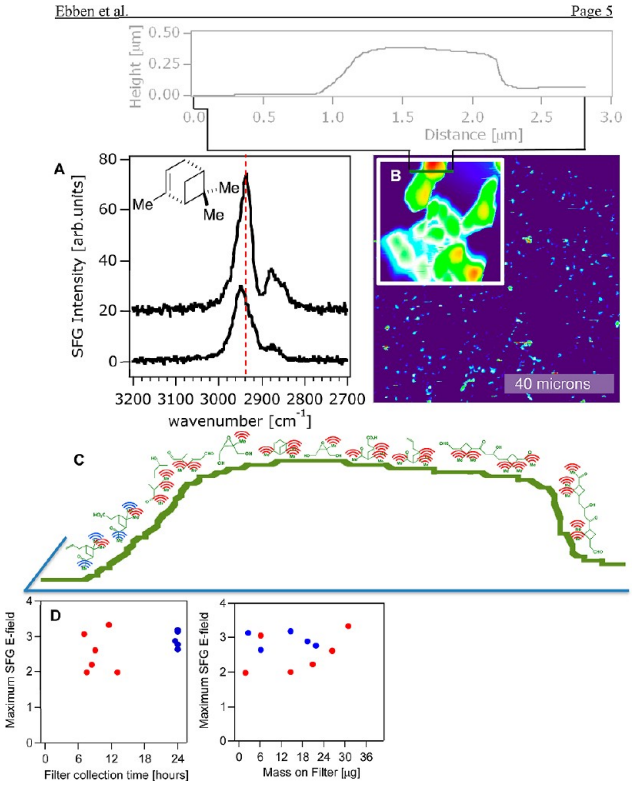

Figure 5. ssp-polarized SFG spectra of α-pinene vapor in contact with a fused silica window (A, top) and α-pinene-derived SOA from the Harvard Environmental Chamber (A, bottom). Contact mode atomic force microscopy images obtained from less than 2 μg of aerosol particle material collected using the PM1 sampler shown in Figure 2A in Southern Finland from 22:00 on 22 June 2010 to 06:30 on 23 July 2010. The AFM images were recorded using a Bioscope II Scanning Probe Microscope with a NanoScope V controller (Digital Instruments) at a resolution of 512 × 512 lines and with V-shaped SNL-10 probes (Veeco) with a 0.12 N/m spring constant and a 16–28 kHz resonant frequency (B). Simplified cartoon of molecules of interest on the surface of a given aerosol particle collected using the PM1 sampler shown in Figure 2 (C). Red and blue oscillators represent asymmetric and symmetric CH stretches, respectively, of the CH_3 groups. (D) Maximum SFG E-field between 2940 and 2960 cm^{-1} obtained from Teflon filters containing the PM1 size fraction collected during HUMPA-COPEC 2010 during the days discussed here as a function of filter collection time (left) and mass on the filter (right).

of (+)-α-pinene exhibits the asymmetric and symmetric methyl CH stretches at 2960 and 2880 cm^{-1}, respectively, as well as a methyl Fermi resonance at 2940 cm^{-1}, which dominates the spectral response. For comparison, the vibrational SFG spectra of *cis*-2-pentene, *n*-hexene, *n*-pentene, cyclohexene, and cyclopentene vapor in contact with an α-alumina optical window, which we analyzed previously,[165] show substantial signal intensity in the symmetric CH stretching region below 2900 cm^{-1}, and this distinguishes them from the terpenes. Although the SFG spectra of cyclohexene and cyclopentene clearly show vinylic CH stretches above 3000 cm^{-1},[165] the olefin CH stretch of (+)-α-pinene is not observed. Other polarization combinations, including those probing vibrational modes oriented perpendicular to the surface normal, do not reveal it either. This observation is attributed to the fact that the Raman polarizability and infrared transition moments of this single olefin CH oscillator are weak. Figure 5A shows that the ssp-polarized SFG spectrum of synthetic SOA particles prepared at the HEC is shifted by about 20 cm^{-1} toward 2950 cm^{-1}, the tell-tale frequency of the Fermi resonance of the CH_3 symmetric stretch with a CH_3 bending overtone typical of CH_3 groups on long-chain aliphatic molecules.[166−168] No new spectral features appear, which indicates that the particle material contains CH oscillators that produce SFG responses that are similar to those of α-pinene vapor in contact with a fused silica window.

Isotope-editing of the methyl groups of α-pinene should be very informative for the structural analysis of organic material derived from α-pinene. One important question is if the three methyl groups in α-pinene and the organic aerosol particle material derived from it add coherently, or if there is one type of methyl group that dominates the SFG response. Future work that is planned within our program will involve stepwise isotope editing. Such synthetic approaches will allow us to spectroscopically assign these very important molecules, whose vibrational responses in the CH stretching region have remained sparsely studied until now, and to produce important experimental spectroscopic benchmarks for their theoretical studies.

Until we have prepared the relevant isotope-edited compounds, we invoke mass spectrometric data collected by others, for instance from the Johnston group,[89,90] which supports the idea that the four-membered ring of α-pinene remains closed upon ozone oxidation. Given the rigidity of this arrangement, strong vibrational coherences and coupling are expected for the CH stretching region, as is evident in the spectra shown in Figure 5A. We generally observe that, when compared to α-pinene, the methyl groups of aliphatic hydrocarbons, which possess much floppier carbon backbones than α-pinene, yield significantly less SFG signal intensity in the frequency region corresponding to the methyl asymmetric stretches and Fermi resonances.[165] This then leads us to propose that the synthetic organic material prepared at the HEC consists of monomers, dimers, or possible oligomers having repeating units of four-membered rings with two methyl groups, similar to what is shown in Figure 3.[169]

IX. NATURAL AEROSOL PARTICLES FORMED IN α-PINENE-RICH AIR IN SOUTHERN FINLAND

A. Some Basic Considerations Regarding Vibrational SFG Signals from Organic Aerosol Particles. Before discussing the SFG spectra of the aerosol particles collected at the SMEAR II field-sampling site, we briefly discuss where the ssp-polarized SFG signals come from when SOA particles are studied. We re-emphasize here that it is the oscillators located in noncentrosymmetric environments that produce the ssp-polarized SFG signals discussed in the majority of the work presented. This distinguishes the method from the various forms of aerosol analytics discussed in section VI, which suggest that organic aerosol particles contain multiple organic species, including the ones shown in Figure 3. Of these many species, the surface-localized species that are also part of a nonzero average net orientation distribution produce the ssp-polarized SFG responses discussed here. As such, we generally expect SFG spectra of organic aerosol particles be much less spectroscopically congested that those obtained from noncoherent spectroscopic methods, in which every oscillator contributes to the spectrum.

Contact mode atomic force microscopy (AFM) images of the PM1 size fraction of aerosol particle material transferred onto a silicon wafer from one of the Teflon filters collected at the HUMPPA-COPEC-2010 site are shown in Figure 5B. This filter had been collected during the night from 22 to 23 July 2010 for a

dx.doi.org/10.1021/jp302631z | J. Phys. Chem. A 2012, 116, 8271−8290

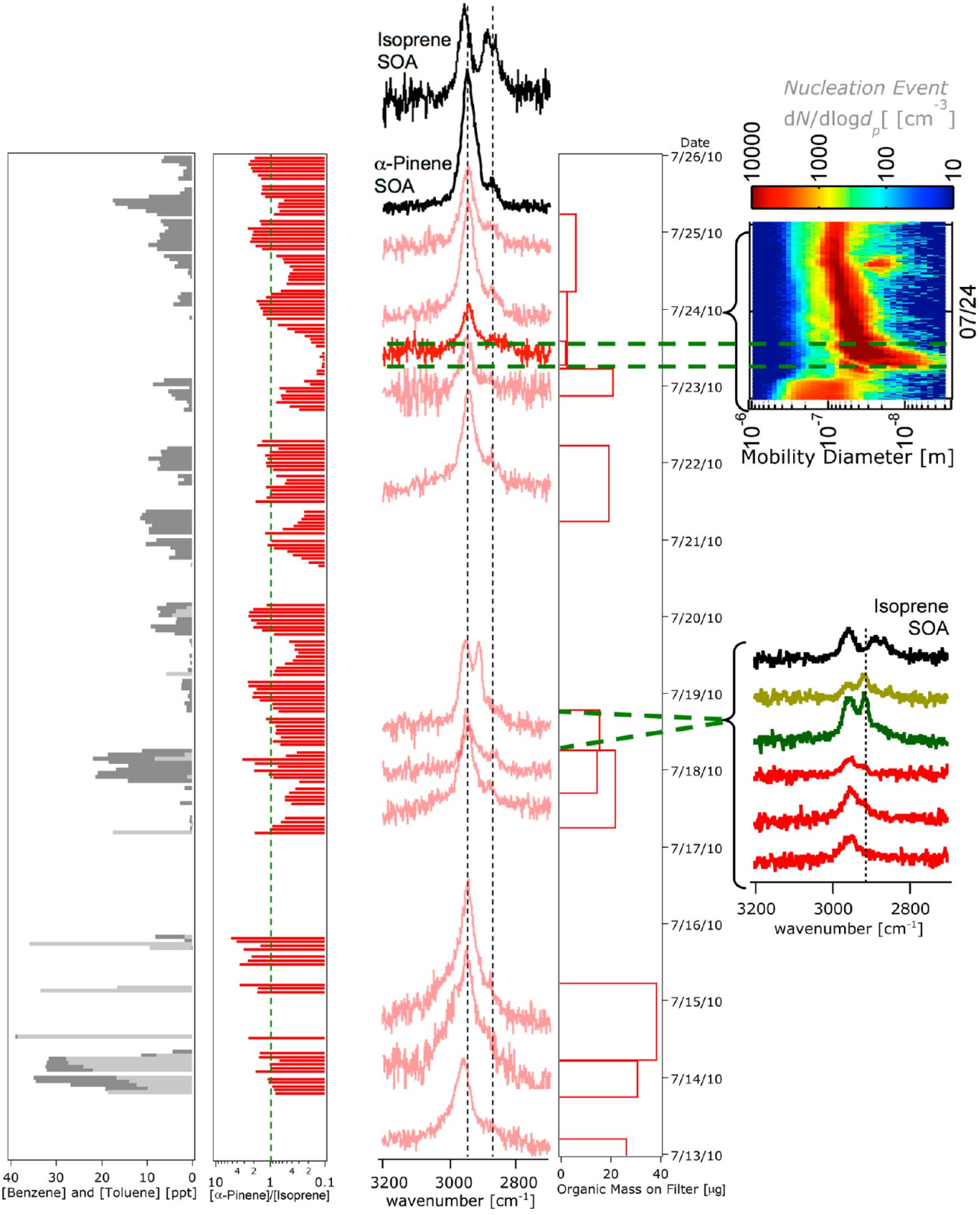

Figure 6. Concentrations of benzene (dark gray sticks to zero) and toluene (light gray sticks to zero), α-pinene-to-isoprene ratio (red sticks to zero), and ssp-polarized vibrational SFG spectra of a fused silica window in contact with a Teflon filter containing aerosol particles with diameters below 1 μm collected in Southern Finland during the HUMPPA-COPEC-2010 field intensive and corresponding gas phase concentrations of isoprene and α-pinene. Top inset: electrical mobility equivalent diameter and particle number density recorded during the nucleation event that occurred from 23 to 24 July 2010. Bottom inset: five ssp-polarized spectra obtained from five spots of the filter collected on 18 July 2010 showing one (red spectra) and two (dark and light green spectra) peaks, and reference SFG spectrum of isoprene-derived SOA prepared at the HEC.

total of 8.5 h, and contained ca. 20 μg of material in the PM1 size fraction. The AFM images of the material on the silicon wafer show irregularly shaped particles that have a height of up to 0.5 μm and diameters ranging from several hundred nm to

dx.doi.org/10.1021/jp302631z | J. Phys. Chem. A 2012, 116, 8271−8290

around one micrometer that are randomly arranged in clusters and aggregates on the substrate. Organic molecules such as α-pinene and isoprene and their oxidation products have a size of about 1 nm and possess low symmetry, such as C_1. For a pancake-shaped particle, such as the one shown in Figure 5B, the ssp-polarized SFG response is mainly due to molecules located on top of the particle that have components of their vibrational transitions moments oriented perpendicular to the top of the particle surface (Figure 5C). Molecules located on the side of the particle that have components of their vibrational modes oriented parallel to the particle surface will contribute to the ssp-polarized SFG response as well. Given that many more molecules are localized on the large flat portion of the particle than on the side, the ssp-polarized SFG responses are likely to originate mainly from the vibrational modes that are associated with those molecules that reside on the flat portion of the particle and that have components that are oriented perpendicularly to that portion of the particle surface. Although a systematic study of this situation is beyond the scope of and relevance to this work, it is planned as part of our efforts in applying nonlinear optics to aerosol particles resting on flat impactor surfaces.

Figure 5D shows the maximum SFG E-field between 2940 and 2960 cm^{-1}, assigned tentatively to the methyl Fermi resonances and/or the asymmetric methyl stretches, recorded for the Teflon filters that contained the PM1 size fraction collected during HUMPA-COPEC 2010 during the days discussed below as a function of filter collection time and mass on the filter. We find that the *E*-field does not uniformly increase with collection time or with mass on the filter, even though the filters that were collected for shorter time (shown in filled red circles in Figure 5D) may have somewhat higher *E*-field values for filters containing more mass. We also note that the distribution of the SFG E-field responses is more narrow for 24 h vs 6−12 h collection times. We interpret the data presented in Figure 5D such that the ssp-polarized SFG responses discussed here are mainly due to the organic species on the aerosol particle surfaces, and that even lightly loaded filters already contain enough aerosol particle material to cover most of the filter. A 1 cm^2 Teflon filter containing a mass loading of 20 μg, such as the one examined by AFM after transferring some of its nonsticky portion onto a silicon wafer, would be coated by an organic layer that is on average 133 nm. This estimate assumes a density of the organic material of 1.5 g/cm^3 and uniform deposition on the filter. We conclude that the SFG detection limit should allow for the analysis of filters containing much smaller mass loadings, as is indeed observed when investigating a filter collected during an aerosol particle nucleation event, during which the cleanliness of the air above the forest approaches that of some clean room conditions.

B. Spectroscopic Analysis and Interpretation. Figure 6 shows a series of eleven ssp-polarized SFG spectra, each averaged from SFG spectra obtained from one to six individual spots on eleven PM1 filters collected between 13 July 2010 and 25 July 2010 at Hyytiälä, along with the ssp-polarized SFG spectra obtained for α-pinene- and isoprene-derived SOA material synthesized at the HEC. The SFG spectra obtained from the field-collected particles are remarkably similar to that of the α-pinene model system, even though there are several samples that were collected on days during which isoprene concentrations exceeded α-pinene concentrations by a factor of up to 2 or 3 for multiple hours, as indicated by the vertical green dashed line. Signal contributions in the aromatic CH stretching region are generally weak if present at all under the experimental conditions employed here, which is consistent with the 10-fold concentration excess of the terpenes over benzene and toluene, the typical markers for fossil burning activities, during this first half of the HUMPPA-COPEC campaign. Future work will specifically cover the full range of the aromatic CH stretching region to further investigate it for the presence of aromatic compounds.

All the PM1 filters studied here are very uniform in their spectral response, i.e., the frequencies that correspond to the maximum SFG signal intensity, except for one, which was collected from 06:00 to 18:00 local time on 18 July 2010. Two out of five ssp-polarized SFG spectra obtained from five different spots on this filter, which are also shown in Figure 6, are quite dissimilar from the other three. Their average exhibits the presence of one additional strong peak at 2915 cm^{-1}, which is not observed in the other spectra we recorded. This finding led us to investigate whether the SFG signal at 2915 cm^{-1} might be a signature of isoprene in the particles, as isoprene was quite abundant during the time of particle collection. However, the ssp-polarized SFG spectra of isoprene-derived synthetic aerosol particles prepared at the HEC are at variance with those obtained from the filter collected on 18 July 2010. We tentatively attribute the new spectral feature to (i) the possible presence of one or more of the compounds shown in Figure 3, (ii) anthropogenic compounds such as benzene or toluene, which were both relatively high in concentration during the day preceding collection of the filter that exhibits the additional SFG spectral feature at 2915 cm^{-1}, or (iii) emissions associated with sawmill activities occurring downwind from the sampling site in the early morning hours of 18 July 2010 (please see section VIIIC).

Finally, we note that work by Barnette et al.[170] shows comparable SFG spectra, recorded in humid ambient air, for crystalline cellulose in biomass, including woody cells of wood chip samples from Scandinavian birch (*Betula pendula*). Although the presence of cellulose in the PM1 particle samples collected during HUMPPA-COPEC-2010 is not known, high organic hydroxyl group concentration associated with vegetative detritus source types apparent in the positive matrix factorization analysis of particles collected at Whistler forest in southwest Canada[171] may be due to cellulose and related compounds. Such compounds are likely to be present in the tail of the supermicrometer size mode that contributes to the PM1 size fraction examined here in a minor way and are the subject of some of our planned future work.

C. Nucleation Event. On the morning of 23 July 2010, the field site experienced an aerosol particle nucleation event, during which fresh air from the Arctic entered the area with lower concentrations of terpenes. With the air being practically void of SOA particle precursors, the aerosol particle number density dropped from more than 1000 particles per cm^3 to just a few tens of particles per cm^3 during the early morning hours. In fact, the particle concentration during such an event can approach that of some lower level clean room conditions. This feature is typical for the Hyytiälä measurement site during the springtime[172] but occurs rarely during the summer. Terpene production by the forest continued, and thus the aerosol particle population built up over the course of the day to about 1000 particles per cm^3, with sizes ranging from 50 to 100 nm. The absence of the larger particles is critical for nucleation, because the terpene oxidation products would otherwise condense on the large surface area offered by the existing particles rather than forming new particles.

Although the spectroscopic analysis of the small number of nanometer-sized particles available for collection during the time of a nucleation event is a major challenge for most spectrochemical methods, it is possible through the strong signals generated in the vibrational SFG spectroscopy of organic aerosol particles. Specifically, Figure 6 shows the ssp-polarized SFG spectrum obtained from particles collected from the start of the nucleation event (06:00 local time, as indicated by the horizontal dashed line) through 14:00 of the same day. This spectrum was recorded in the same fashion as the other spectra shown in Figure 6, namely by using 2 min per spectral acquisition, repeated seven times to increase the signal-to-noise ratio. Though being the least intense SFG spectrum of the set, which is consistent with the low estimated mass of organic material on the filter (<2 μg), the spectral signature at 2945 cm^{-1} and the shoulder at 2880 cm^{-1} are clearly visible.

The sum of (+)- and (−)-α-pinene concentration at the beginning of the nucleation event at 06:00 on 23 July 2010 was 28 ppt whereas it was 243 ppt for isoprene. This low ratio of α-pinene-to-isoprene concentrations persisted throughout the day, possibly attributable to conditions such as low temperature and high radiation that favors isoprene emissions relative to the other terpenes. For instance, at 14:00, the stop-time for the filter whose ssp-polarized SFG spectrum is underlined by the green horizontal line, the α-pinene-to-isoprene concentration ratio had decreased to just 0.17. Finally, by 22:00 of the same day, the ratio of α-pinene-to-isoprene concentrations had increased back to above 1.0. Yet, though isoprene concentrations far exceeded those of α-pinene during the daytime of 23 July 2010, isoprene-like SFG spectral signatures were not obtained from the PM1 size fraction of collected aerosol particles. Instead, the ssp-polarized SFG spectra are remarkably similar to those obtained throughout the majority of the two-week period studied. This result suggests that the surfaces of the SOA particles that were formed during the nucleation event contain, at least as probed by vibrational SFG spectroscopy, of derivatives of α-pinene and not of isoprene. This interpretation is consistent with the notion that isoprene is a rather inefficient SOA source under the conditions encountered at the sampling site in Southern Finland. We conclude from the data presented in Figure 6 that in as far as the SFG spectra presented here probe the chemical composition of aerosol particle surfaces, the α-pinene-derived organic material synthesized at the HEC is a reasonable model for analyzing the surfaces of organic aerosol particles formed during the summertime in Southern Finland that represents around 90% of organic material collected on the filters examined here by SFG.

D. Molecular Chirality and the Aerosol Particle and Gas Phases. In 2009, we published an article discussing the possible role of atmospheric heterogeneous stereochemistry in aerosol chemistry and physics.[173] Although chirality effects in terpene biosynthesis[174] as well as in reverse micelles, which may be invoked as aerosol particle models,[175,176] have been studied for quite some time now,[177] the topic of chirality in atmospheric chemistry is now just emerging,[178,179] with several groups, including the collaborative team of coauthors,[159,160,173] studying specifically chirality in organic aerosol particles.[180−183] Using the psp-polarization combination,[184] which not only accesses several elements of the nonlinear susceptibility tensor, including the χ_{xyz} tensor element that is uniquely nonzero for all chiral species, but also may include achiral contributions, we obtained nonzero vibrational SFG signatures from aerosol particles collected during the summer in Southern Finland in the PM1 size fraction (Figure 7A). Specifically, we find a single vibrational resonance at 2960−2950 cm^{-1}, which agrees well with the one we obtained from synthetic SOA particle samples prepared at the HEC from varying ratios of (+)- and (−)-α-pinene using a related polarization combination.[159] Aerosol particles collected in March 2011, the early spring following the HUMPPA-COPEC-2010 field intensive, show minor to negligible SFG signals, even though the ssp-polarized SFG spectrum, which samples achiral contributions, shows the presence of α-pinene-derived organic material (Figure 7B). Future studies will require the springtime determination of the enantiomeric excess (EE) of (+)- over (−)-α-pinene in the gas phase to assess whether the absence of a chiral SFG signal in the aerosol particles collected in March 2011 indicates if the particles on the filter samples do not contain chiral species or if they contain racemates.

Prior analysis of events occurring during the HUMPPA-COPEC field campaign identified two days during which the field measurement site was downwind from operating sawmills,[3] namely 18 July 2010 and 6 August 2010. It has been previously established that mechanical damage to pines is associated with an increase in the ratio of (+)- to (−)-α-pinene in the gas phase.[185] Due to the fact that the boundary layer becomes shallow and emissions from the freshly sawn wood are advected most effectively to the site late at night, the (+)-α-pinene enantiomeric excess (EE) in the air at the field measurement site was around 50% during the early morning hours, as indicated by the white asterisks in Figure 7A. The top psp-polarized SFG signal shown in Figure 7A was obtained from particles that were collected over an 8 h period following the 6 August 2010 sawmill event. We interpret the strong psp-polarized SFG response to be a signature of the large excess of (+)-α-pinene in the air that apparently had enough time to be incorporated into the collected aerosol particles. The middle spectrum was obtained from particles collected over a 24 h period while there was no sawmill activity and also relatively low EE of (+)-α-pinene in the air, and it exhibits minor psp-polarized SFG intensity. Finally, the bottom spectrum was obtained from particles collected during a 12 h period which included pronounced saw mill activity, albeit on its tail end, and also pronounced EE of (+)-α-pinene in the air during times preceding the saw mill event, and its psp-polarized SFG intensity is between that of the two spectra above it.

We interpret these findings as follows: Figure 7A shows that EEs of (+)-α-pinene in air below 20% or so lead to minor psp-polarized SFG responses unless events associated with much higher EE values precede particle collection by several hours. When particle collection coincides with high EE values, then the psp response is appreciable as well, which is consistent with our previously published model study.[159] If the psp-polarized SFG spectra are dominated by the vibrational responses of chiral molecules, then it should be possible to connect (in time) the enantiomeric composition of the particles with the enantiomeric composition of the gas phase (Figure 7C). One could therefore use chirality as a marker, or label, for determining the rates of aerosol formation from gas phase constituents. Use of such a "chiral marker" could then help answer whether aerosol particles present in air at a certain hour on a certain day were formed from VOCs that were present in air 3, 6, 12, or 24 h earlier because the EE varies over this time frame. The fact that the (+)-α-pinene EE is anticorrelated with the diel cycle (Figure 7C) makes the concept of a "chiral marker" a real possibility for understanding the time scales associated with aerosol particle formation. Simply put, chirality can be used to mark a gas phase condition (in this

dx.doi.org/10.1021/jp302631z | J. Phys. Chem. A 2012, 116, 8271−8290

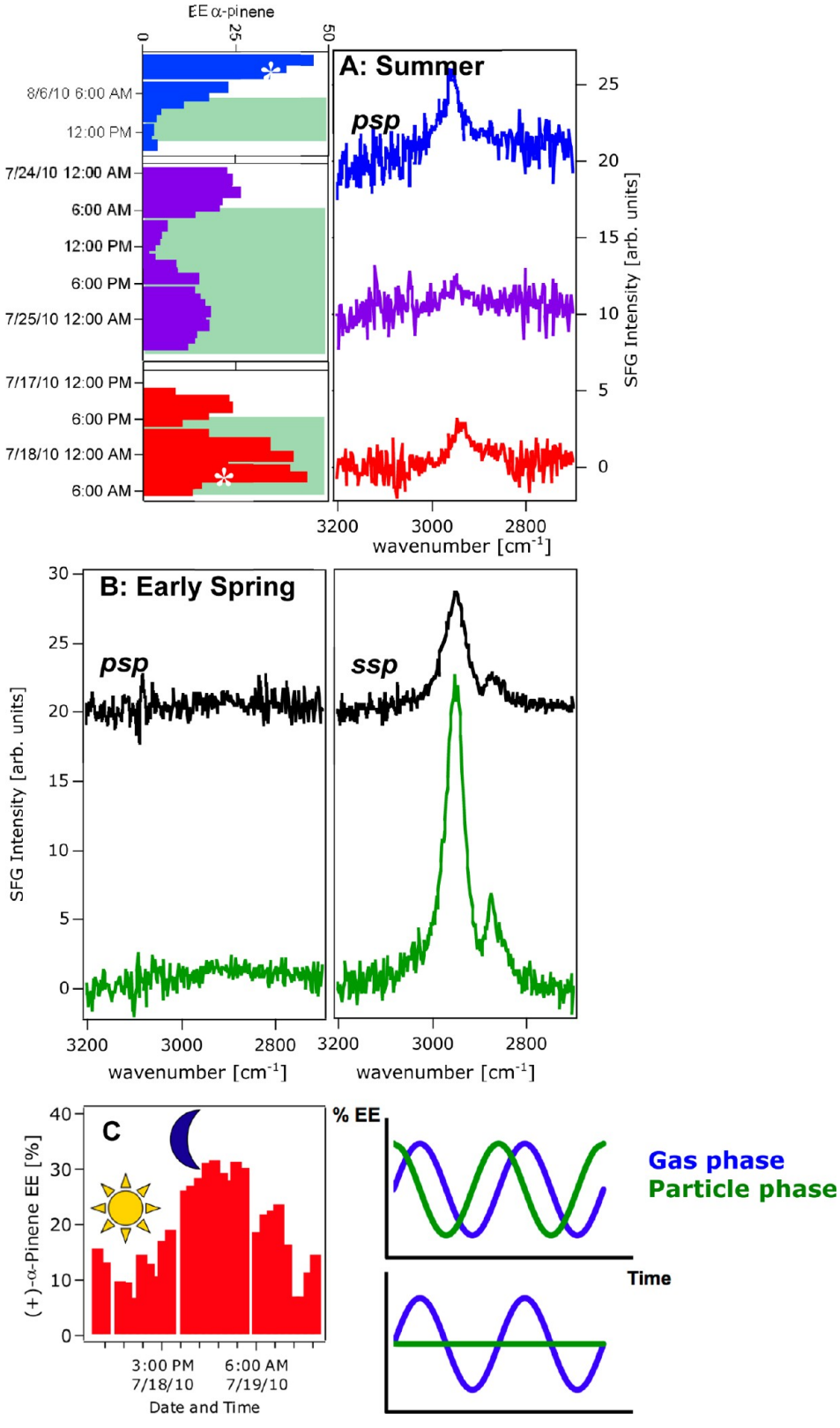

Figure 7. (A) Enantiomeric excess of (+)-α-pinene in the gas phase and corresponding psp-polarized vibrational SFG spectra of aerosol particles collected in the PM1 size range during the times indicated in green, with asterisks marking high EE values associated with advection of emissions from the freshly sawn wood to the field measurement site. (B) psp-polarized (left) and ssp-polarized (right) SFG spectra obtained from particles collected on 23 (top) and 25 (bottom) March 2011. (C) (+)-α-Pinene enantiomeric excess (EE) as a function of hour in the day of 18 to 19 July 2010 (left) and concept for a chiral carbon tracer to connect aerosol gas phase with aerosol particle phase chemistry (right). Please see text for details.

case, EE), and the SFG readout could then identify when particles with that EE begin to form (Figure 7C).

Figure 7B shows that psp-polarized SFG spectra of particles collected in the PM1 size fraction during the early spring at the

dx.doi.org/10.1021/jp302631z | J. Phys. Chem. A 2012, 116, 8271−8290

same field site yield little to no signal above the noise. Work by Eerdekens et al.[186] shows generally smaller monoterpene concentrations in the 0.06−0.18 ppbv during the colder period of their early April 2005 study than in this present work (Table 1). A similar study by Liao et al.[187] carried out during several periods including early March 2007 shows monoterpene concentrations between 0.01 and 0.1 ppbv, with episodic (hour-long) concentration spikes rising as high as 1 to 2 ppbv. Those conditions are likely comparable to the conditions of 23 and 25 March 2011, when the particles whose SFG spectra are shown in Figure 7B were collected. Despite the smaller overall monoterpene concentrations in early Spring, the filters did indeed contain organic aerosol particle material, as evidenced in the ssp-polarized SFG spectra shown in the right spectrum of Figure 7B. We conclude that the aerosol particle samples here that were collected in the early Spring 2011 contain either racemates or achiral species or both. Alternatively, the chiral enrichment of the chemical composition could be too small for SFG spectroscopy to detect, which is the subject of future work in the form of careful limit-of-detection studies involving smog chamber models at the HEC. Future work will also focus on the use of polarization combinations which probe only the chiral components of the particles, with no achiral contributions.

X. AEROSOL PARTICLES COLLECTED FROM AIR RICH IN ISOPRENE (AMAZONIA)

To contrast atmospheric aerosol chemistry and physics in the boreal forest with that of tropical forests, we present in this section results obtained by vibrational SFG from aerosol particles collected in the central Amazon Basin. Unlike in the previous section, the Amazonian field campaign sampled organic aerosol particles using MOUDIs, so our discussion will center on the spectral analysis of size-resolved aerosol particles. As the chemical reactions for the formation of organic aerosol particles are likely to be dominated by isoprene oxidation by OH radicals (Table 1), we begin by discussing the ssp-polarized SFG spectra obtained from isoprene-derived particles synthesized in 2010 at the HEC and of isoprene vapor in contact with a fused silica window (Figure 8A).[92] Unlike in the case of α-pinene and its oxidation products (Figure 5), the organic material prepared from isoprene oxidation by OH radicals at the HEC (here, ppb levels of OH radicals are used as an oxidant, as described in our published work)[92] is spectrally quite dissimilar from the isoprene precursor: the vinylic CH stretches above 3000 cm^{-1} are clearly observable for isoprene, which also shows asymmetric and symmetric CH stretches at 2950 and 2850 cm^{-1}, respectively, as well as a strong vibrational resonance at 2900 cm^{-1}. The absence of vinylic CH stretches in the SFG spectrum of the isoprene-derived organic material from the HEC is consistent with C=C double bond oxidation. In fact, the appearance of asymmetric and symmetric methyl and symmetric methylene stretches at 2950, 2880, and 2850 cm^{-1}, respectively, and the disappearance of the vinylic CH stretch of isoprene suggest the formation of aliphatic compounds containing methyl groups upon SOA formation.

Panels B and C of Figure 8 show the ssp-polarized SFG spectra of the coarse and fine modes, respectively, of organic aerosol particles collected on nucleopore impactor substrates using a MOUDI operating from 9 April 2008 to 17 April 2008 at the site of the AMAZE-08 campaign described in section II. Figure 8B shows that the particle material in the coarse mode, which samples sizes larger than one micrometer, exhibits many spectral features that are different with each new sample spot on the same filter. For instance, the top three spectra displayed in Figure 8B are obtained from three different spots on MOUDI stage 3, and none resemble one another. The chemical complexity of these particles in the coarse mode that is reflected by their spectral variability is likely due to the presence of primary biological material such as pollen or plant debris in these particles.[68] The three SFG spectra of the particles collected on three spots of the filter holding the next smaller size fraction (1.8 μm) are much more similar to one another but weaker in intensity.

In contrast to what we observe in the coarse mode, the ssp-polarized SFG spectra obtained from submicrometer sized particles (Figure 8C) are roughly invariant with size: for particles with aerodynamic diameter 50% cutoffs of 1.0 μm, 560 nm, and 330 nm, there is little variability in the SFG spectra, at least in the CH stretching region. The isoprene-derived organic material prepared at the HEC and the isoprene precursor exhibit no peak at 2900 cm^{-1}, which is prominent in the fine mode of the field-collected aerosol particle samples. The difference in the SFG responses between the synthetic SOA material and the field-collected particles could be attributed to differences in OH concentration conditions in the chamber and the field,[188] but OH concentrations at the HEC are ca. 7×10^6 OH radicals per cm^3,[11] which compares favorably with the OH concentration range for the central Amazon Basin during the relevant time frame of sample collection. Alternatively, the spectral differences between the chamber- vs the field-derived samples could be due to chemical complexity: as reported by Wenberg and co-workers in 2009,[189] isoprene can undergo photooxidation in the gas phase to produce epoxides. Formation of methyltetrols has been reported as well by Claeys and co-workers,[49,190] and these compounds could be the origin of the spectral features observed in the SFG spectra shown in Figure 8C. However, until we have prepared the proper reference compounds for analysis by SFG spectroscopy, it is not possible for us to confirm the presence of epoxides, tetrols, or related compounds in the isoprene-derived organic material synthesized at the HEC or collected in the central Amazon Basin.

To assess whether the SFG signal intensities depend on the bulk optical properties of the sample material on the various MOUDI stages, we recorded their reflectivity spectra. This experiment was carried out because of the low transmittivity of the MOUDI stage substrates, which are made of nucleopore. Given that the high dilution of just a few micrograms of aerosol particle material over the entire 1 in. area of each MOUDI stage make these measurements challenging, we show in Figure 8C the optical images and reflectivities of a set of MOUDI stages that were collected from 1 May to 10 May 2008 while the rotating motor gearbox was disengaged. This situation fortuitously resulted in enough material under each of the microorifices, as shown in the insets of the bottom five optical images, that reflectivity data could be readily collected using our spectrophotometer while simultaneously providing background reflectivities from uncoated areas, as shown in the gray spectra in Figure 8C. Optical images were obtained using ultralong working distance epiplan-neofluar 10× and 50× objectives with numerical apertures of 0.2 and 0.55, respectively, resulting in a maximum calculated resolution of 1.2 and 0.4 μm, respectively, at 400 nm. The images are detected with a thermoelectrically cooled CCD detector (Princeton Instruments).[191] Optical reflectivities at normal incidence of illumination and detection were obtained using an Ocean Optics spectrophotometer coupled to a Zeiss binocular phototube using the appropriate fiberoptic.

In general, we find that the aerosol particle material on the MOUDI stages appears round or elliptical except for the stage

dx.doi.org/10.1021/jp302631z | J. Phys. Chem. A 2012, 116, 8271−8290

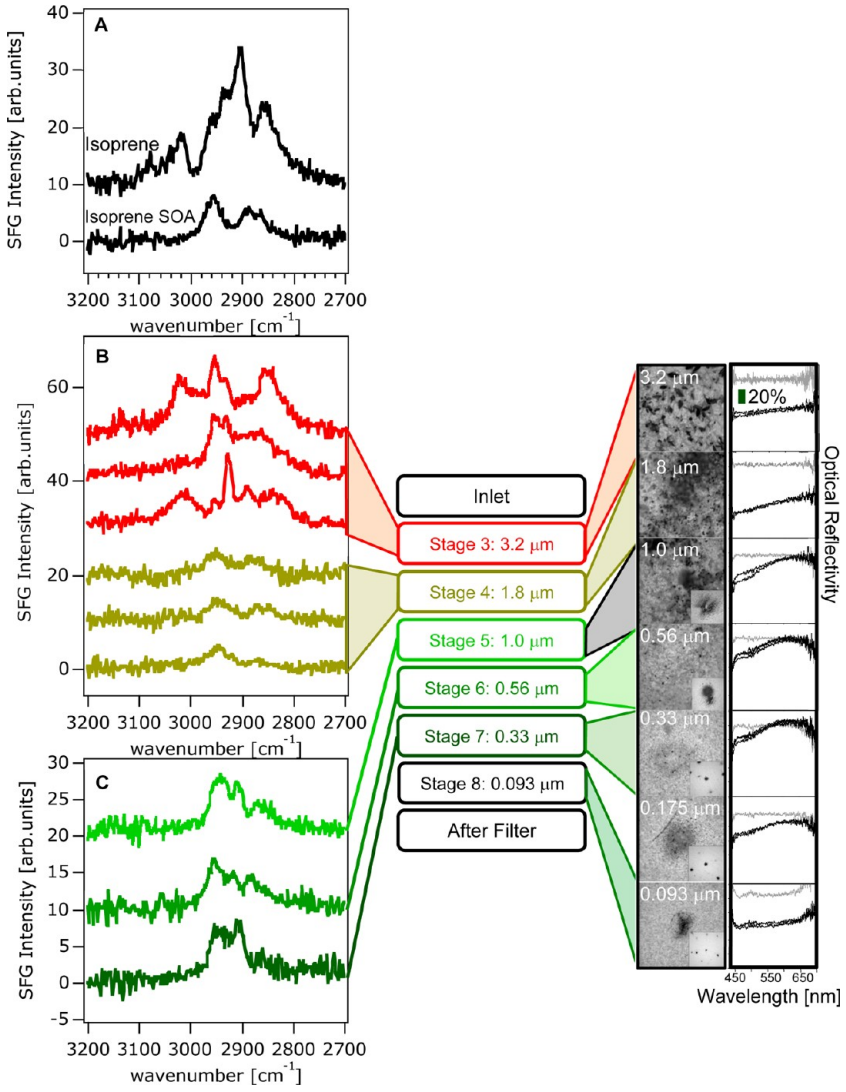

Figure 8. (A) ssp-polarized SFG spectra of isoprene vapor in contact with a fused silica window (top) and of isoprene-derived SOA particles prepared at the Harvard Environmental Chamber (bottom). (B) ssp-Polarized SFG spectra of particles having aerodynamic diameter 50% cutoff sizes of 3.2 μm (red) and 1.8 μm (olive) sized particles collected at tower TT34 and of particles having aerodynamic diameter 50% cutoff sizes of (C) 1.0 μm (top), 560 nm (middle), and 330 nm (bottom) collected at site TT34 in the central Amazon Basin in March 2008. (C, right) Optical images obtained with a 50× objective and 10× objective as shown in the insets of the bottom five images, along with optical reflectivity spectra obtained from six MOUDI stages containing SOA particles of the indicated aerodynamic size range sampled in the central Amazon Basin (right).

selecting the largest sizes, which is likely due to primary emissions from plants, such as pollen. The reflectivity spectra show that the samples become generally more reflective with decreasing size at wavelengths shorter than 600 except for the very last stage (0.093 nm), which is likely due to the fact the material on this stage contains somewhat elevated black carbon content expected from the biomass burning season that starts around that time. At the SFG signal wavelength of ~640 nm, the reflectivities do not appear to change significantly with aerodynamic size range for those stages of which we took SFG spectra, which suggests that optical absorption of the SFG signal at this wavelength contributes negligibly to the SFG signal intensities of the spectra discussed here.

Figure 8C shows that whatever the chemical composition of the submicrometer SOA particles collected in the central Amazon Basin is, the size-invariance of their SFG responses suggests that whatever changes occur in the chemical composition of the particles during growth, the chemical composition of their surfaces is relatively uniform throughout the 100−1000 nm size range, at least as probed by our coherent spectroscopy. The O/C ratios of 0.3−0.5 that are typical for these particles (Table 1)[92] support this interpretation.

XI. AEROSOL PARTICLES FROM ANTHROPOGENICALLY INFLUENCED AIR (BLODGETT FOREST)

We conclude our discussion by contrasting the SFG spectra of aerosol particles collected in Southern Finland and the central Amazon Basin with those obtained from particles collected in Blodgett Forest, CA. The aerosol particles were collected from 1 to 4 July 2009, 4−8 July 2009, 11−14 July 2009, and 25−28 July 2009 with a 2.5 μm cutoff. Back-trajectories for the period of time from 1 to 4 July indicate that the air masses arriving at the site during this time were predominantly from the west and southwest. These air masses passed over the Sacramento Valley before arriving at the sampling site, so there is large potential for anthropogenic influence in this particle sample. Back-trajectories

dx.doi.org/10.1021/jp302631z | J. Phys. Chem. A 2012, 116, 8271−8290

for the sample collected from 25 to 28 July indicate that the air masses present during the formation of these particles were more variable in origin, sometimes originating from the west/southwest and at other times originating from the less populous north.

The ssp-polarized SFG response in the CH stretching region of these particles depends largely on the origin of the air present during their formation. Signal contributions above 3000 cm^{-1}, as seen in the top two spectra of Figure 9, indicate the presence of

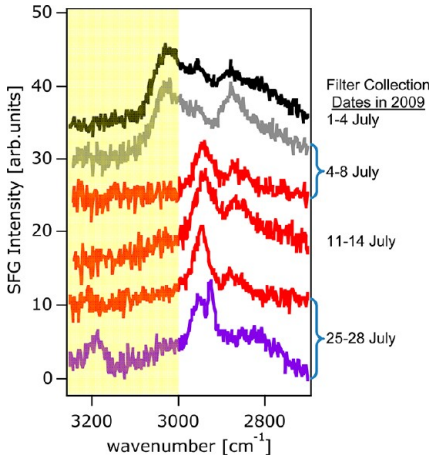

Figure 9. ssp-polarized SFG spectra of particles collected during the following dates: 1−4 July 2009 (top), 4−8 July 2009 (second and third from the top), 11−14 July 2009 (fourth from the top), and 25−28 July 2009 (bottom two) in Blodgett Forest, California.

aromatic material in the particles, which is attributable to anthropogenic emissions such as those produced from fossil fuel burning that were entrained in the air as it moved through the Sacramento Valley toward the sampling location.[192,193] The large nonresonant contributions in the spectra are indicative of highly polarizable materials such as elemental carbon.[194−196]

As seen in Figure 9, one of the spots on the filter collected during July 4−8 2009 yielded a spectrum that is comparable to that of α-pinene SOA. We note that Bouvier-Brown et al. reported that β-pinene is the dominant monoterpene in Blodgett Forest.[12] In our future work, we will characterize β-pinene-derived SOA particle material, which will be synthesized in the HEC. The expectation is that if the four-membered ring with the two methyl groups, which both α- and β-pinene possess, dominates the coherent vibrational SFG response of SOA particles formed from them, then it may not be straightforward to distinguish α- from β-pinene-derived SOA material by SFG.

The SFG spectrum resembling that of the α-pinene SOA reference material synthesized at the HEC is comparable in terms of peak positions to those obtained from aerosol particles collected during 11−14 and 25−28 July 2009 with the exception of the spectrum shown at the bottom of Figure 9. As mentioned above, anthropogenic influences were variable during these days, and the aromatic contributions at 3200 cm^{-1} that can be seen in the bottom spectrum of Figure 9 may be associated with aerosol particles containing emissions from fossil fuel combustion. We conclude from the spectra shown in Figure 9 that anthropogenic influences at the Blodgett Forest sampling sites are readily identified by SFG in the sub-2.5 μm size fraction of aerosol particles collected there, in fact, much more so than in Southern Finland, at least during the time periods studied here.

XII. CONCLUSIONS AND OUTLOOK

In conclusion, we have investigated the surfaces of natural aerosol particles from three different forest environments using vibrational SFG (Figure 10). The experiments were carried out

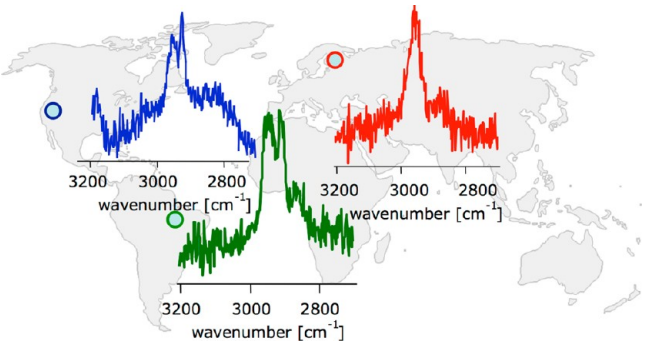

Figure 10. Vibrational SFG spectra in the CH stretching region of aerosol particles from the boreal, tropical, and pine forests discussed in this work.

directly on filter and impactor substrates, without the need for sample preconcentration, manipulation, or destruction. As part of this work, we have shed light on the important first steps leading to SOA particle nucleation and growth from α-pinene by showing that, at least as viewed by vibrational coherent spectroscopy, the chemical composition of the surface species is close to size-invariant over the size range studied here. We also introduced the concept of molecular chirality as a chemical marker that could be useful for quantifying how chemical constituents in the SOA gas phase and the SOA particle phase are related in time. In addition, we have shown how micrograms of SOA particle material on PM1, PM2.5, and MOUDI collection filters are readily analyzed by vibrational sum frequency spectroscopy in a nondestructive fashion that does not require pulling a vacuum on the sample.

In general, we find that the surfaces of particles from boreal and pine forests (Finland and California) produce ssp-polarized SFG responses that are quite comparable to those produced by the surfaces of synthetic α-pinene-derived SOA particles collected at the HEC. These responses are currently attributed to the asymmetric CH stretches and Fermi resonances from the two methyl groups located on the bridge of α-pinene, which are presumably strongly coupled to produce the intense coherent signals we observe, and ongoing work using isotope-edited α-pinene will further help in this spectral interpretation. It is important to reflect on why an environment as complex as the Finnish boreal forest[197] would yield such uniform SFG responses as the ones we show in Figure 6. One reason for such a uniform nonlinear optical response could be the dominance of a few highly coupled asymmetric methyl CH oscillators over a majority of poorly coupled or disordered oscillators that would constitute a largely acrystalline material within the surface environment of the particles. As such, we are now exploring nonlinear optics to evaluate the phase state of organic aerosol particles in terms of their crystallinity. In addition, we learned that chirality may be useful to quantify the time scales that it takes for gas phase species to be incorporated into the SOA particle phase, and that some anthropogenic influences, such as sawmill activity, may be assessed using this important molecular property as well.

Our findings also show that although we do not yet know what the molecular species are that contain the CH oscillators

dx.doi.org/10.1021/jp302631z | J. Phys. Chem. A 2012, 116, 8271−8290

producing the SFG responses of aerosol particles collected in the tropical forest (central Amazon Basin), the chemical composition of the fine mode particles (<1 μm) is remarkably uniform as probed by vibrational SFG spectroscopy (Figure 8). It therefore appears that although organic aerosol particles from the boreal and tropical forest environments are different in their chemical composition, as probed by SFG, they are uniform for each forest environment in chemical composition in the fine mode, again as probed by SFG.

The aerosol particles collected in the ponderosa pine forest show clear anthropogenic influences, which are readily and much more discernible (Figure 9) by SFG than for particles collected in Southern Finland. Extensive reference libraries will aid in the further spectral interpretation. Finally, we have described how the combination of multiple disciplines, such as aerosol science, advanced vibrational spectroscopy, meteorology, and chemistry can be highly informative when studying particles collected during atmospheric chemistry field campaigns, such as those carried out during AMAZE-08, HUMPPA-COPEC-2010, or BEARPEX-2009, and when they are compared to results from synthetic model systems such as the HEC.

Future work will capitalize on the spectroscopic advances described here and be geared toward the study of synthetic putative SOA particle components such as those shown in Figure 3 to pursue detailed spectroscopic assignments by vibrational SFG. To this end, we are in the process of preparing and studying deuterium-labeled SOA particle precursors to fast-forward, in terms of mechanistic studies, through the SOA particle formation process, and to further understand the role of molecular chirality in atmospheric chemistry. In addition, we will also focus our attention on spectroscopic regions of interest other than the CH stretching region. These frequency regions include the CO, CS, CN, CP and the PO, NO, and SO stretching regions, which have been recently studied by Roke and co-workers in the carbonyl stretching region, specifically using microemulsions,[198] and by Allen and co-workers in the SO[199] and PO[200] stretching regions using macroscopically flat aqueous surfaces. In addition, Yan and co-workers investigated the chirality of interfacial protein structures related to plaque formation in the NH stretching region.[201] These new experiments will provide critically needed chemical speciation information regarding the various functional groups associated with SOA particle material.

We conclude this work by stating that the experiments described here would not be possible without the unique sensitivity of vibrational SFG spectroscopy to molecular structure, to environments where symmetry is broken, and to the chemical identity of the oscillators of interest. The ultimate goal of this work is to connect the molecular insight gained from the vibrational SFG studies to the climate-relevant physical and chemical properties of aerosol particles, which we will achieve by tightly integrating field and laboratory studies. It is our expectation that nonlinear optics will become an important and highly sensitive spectroscopic analysis tool for studying the fundamental molecular aspects of atmospheric aerosol particles, be they of anthropogenic or natural origin.

AUTHOR INFORMATION

Notes

The authors declare no competing financial interest.

Biographies

Carlena J. Ebben received her B.S. in Chemistry from Marquette University in 2009, where she worked with Scott Reid. She is currently a Ph.D. student at Northwestern University and an NSF Graduate Research Fellow in Franz Geiger's group, studying chirality in organic aerosol chemistry using vibrational sum frequency generation.

Mona Shrestha, originally from Nepal, graduated with a B.A. in Chemistry and Environmental Science from Wesleyan College, GA. She is currently working towards her Ph.D. in Chemistry with Franz Geiger at Northwestern University. Her research focuses on studying the surface composition of atmospheric aerosol particles employing vibrational spectroscopy.

Imee S. Martinez is a graduate of the University of the Philippines who earned her Ph.D. with Steve Baldelli at the University of Houston in 2010, where she worked on vibrational sum frequency spectroscopic studies of the surfaces of ionic liquids as a Welch Foundation Fellow. Her work at Northwestern focused on nonlinear optical studies of secondary organic aerosol particles.

Ashley L. Corrigan received her B.A. in biochemistry from University of San Diego in 2009 where she worked under the advisement of David DeHaan, and she is currently a graduate student at University of California, San Diego working with Lynn Russell.

Amanda A. Frossard is a 4th year Ph.D. graduate student at Scripps Institution of Oceanography at the University of California, San Diego. She studies the composition and concentration of submicrometer organic aerosol particles in marine environments using Fourier transform infrared (FTIR) spectroscopy.

Wei W. Song is a Ph.D. student at the Max Planck Institute for Chemistry, Atmospheric Chemistry Department, in Mainz, Germany. She joined the Jonathan Williams group in 2007 and is working on the enantiomeric and nonenantiomeric biogenic VOCs emissions at leaf and canopy scales.

David R. Worton received his B.Sc degree in Chemistry from the University of Nottingham in 1999 and his Ph.D degree in Atmospheric Chemistry in 2006 from the University of East Anglia under the supervision of William Sturges. In 2006 he joined Allen Goldstein's group at the University of California, Berkeley, as a postdoc. Since 2009 he has been a research specialist in Goldstein's group and a research associate at Aerosol Dynamics Inc. specializing in the developing of new instrumentation to speciate organic compounds in atmospheric aerosols.

Tuukka Petäjä is the leader of the Aerosol Measurements research group at the University of Helsinki, Finland. He is focused especially on extending the measurement range down to molecular sizes utilizing both traditional aerosol instrumentation and mass spectrometric methods, which are essential for studying new particle formation. Petäjä has coordinated field experiments and activities on all seven continents

Jonathan Williams is an atmospheric chemist. He completed his BSc and Ph.D. at the University of East Anglia, England, and after working as a postdoctoral researcher at the NOAA Aeronomy laboratory in Boulder, USA, he became a research group leader at the Max Planck Institute for Chemistry, Germany, with a focus on the investigation of the chemistry of volatile organic compounds (VOC) in the atmosphere. He has participated in many international field campaigns on aircraft, ships and at ground stations.

Lynn M. Russell is Professor of Atmospheric Chemistry at the Scripps Institution of Oceanography at the University of California, San Diego. Her research interests include atmospheric aerosols and their interactions with clouds, and her recent work has focused on distinguishing the contributions of biogenic and man-made sources to organic particles in the atmosphere.

Markku Kulmala directs the Division of Atmospheric Sciences at the Department of Physics and has served as a professor at the University of Helsinki since 1996. Kulmala also acts as Director for the Centre of Excellence, appointed by the Academy of Finland (Research Unit on Physics, Chemistry, and Biology of Atmospheric Composition and Climate Change), and for the Nordic Centre of Excellence (Biosphere-Atmosphere-Cloud-Climate Interactions, BACCI) as well as for the NorFa Graduate School (Biosphere-Carbon-Aerosol-Cloud-Climate Interactions, CBACCI).

Allen H. Goldstein received his B.S. in chemistry and B.A. in politics from the University of California at Santa Cruz (1989), and his M.S. (1991) and Ph.D. (1994) in chemistry from Harvard University. He joined the faculty at the University of California at Berkeley in 1995, and is currently a Professor in the Department of Environmental Science, Policy, and Management and the Department of Civil and Environmental Engineering.

Paulo Artaxo is professor of environmental physics at the University of São Paulo, Brazil. As one of the coordinators of the Large Scale Biosphere-Atmosphere Experiment in Amazonia, he helped to unveil the complex mechanisms that govern aerosol-cloud interactions, quantifying how aerosol particles influence carbon cycling and the radiation budget in Amazonia.

Scot T. Martin received his B.S. at Georgetown University and his Ph.D. in Physical Chemistry at Caltech as a DOE predoctoral Fellow with Michael Hoffmann, and he completed a NOAA Postdoctoral Fellowship in Climate and Global Change at MIT with Mario Molina. He is the Gordon McKay Professor of Environmental Chemistry in the School of Engineering of Applied Sciences and the Department of Earth and Planetary Sciences at Harvard University.

Regan J. Thomson was born in New Zealand and obtained his Ph.D. in Chemistry at The Australian National University, Canberra, in 2003. After postdoctoral studies at Harvard University, he joined the faculty at Northwestern University in 2006. His research interests are centered on the synthesis and study of natural products.

Franz M. Geiger is a native of Berlin, Germany, where he received his Vordiplom from the Technische Universität. After his Ph.D. with Janice Hicks at Georgetown University as a NASA Predoctoral Fellow in Earth Systems Sciences, and a NOAA Postdoctoral Fellowship in Climate and Global Change at MIT with Mario Molina, he arrived at Northwestern University in 2001, where he is currently the Irving M. Klotz Professor of Physical Chemistry. Geiger studies chirality in cloud chemistry and physics with vibrational sum frequency generation and second harmonic generation applied to natural and synthetic aerosol particles.

REFERENCES

(1) IPCC, 2007: Summary for Policymakers. In *Climate Change 2007: The Physical Science Basis. Contribution of Working Group I to the Fourth Assessment Report of the Intergovernmental Panel on Climate Change*; Cambridge University Press: Cambridge, U.K., 2007.

(2) IPCC *Climate Change 2001: The Scientific Basis. Contribution of Working Group I to the Third Assessment Report of the Intergovernmental Panel on Climate Change*; Cambridge University Press: New York, 2001.

(3) Williams, J.; Crowley, J. N.; Fischer, H.; Harder, H.; Martinez, M.; Petaja, T.; Rinne, J.; Back, J. B.; Boy, M.; Dal Maso, M.; et al. *Adv. Chem. Phys.* **2011**, *11*, 10599.

(4) Rinne, H. J. I.; Guenther, A. B.; Greenberg, J. P.; Harley, P. C. *Atmos. Environ.* **2002**, *36*, 2421.

(5) Lluisa, J.; Penuelas, J. *Am. J. Botany* **2000**, *87*, 133.

(6) Penuelas, J.; Lluisa, J. *Biologia Plantarum* **2001**, *44*, 481.

(7) Climate Change 2007: *The Physical Science Basis*; Cambridge University Press: Cambridge, U.K., 2007.

(8) Riipinen, I.; Pierce, J. R.; Yli-Juuti, T.; Nieminen, T.; Hakkinen, S.; Ehn, M.; Junninen, H.; Lehtipalo, K.; Petaja, T.; Slowik, J.; et al. *Atmos. Chem. Phys.* **2011**, *11*, 3865.

(9) Martin, S. T.; Andreae, M. O.; Althausen, D.; Artaxo, P.; Baars, H.; Borrmann, S.; Chen, Q.; Farmer, D. K.; Guenther, A.; Gunthe, S. S.; et al. *Atmos. Chem. Phys.* **2010**, *10*, 11415.

(10) Worton, D. R.; Goldstein, A. H.; Farmer, D. K.; Docherty, K. S.; Jimenez, J. L.; Gilman, J. B.; Kuster, W. C.; de Gouw, J.; Williams, B. J.; Kreisberg, N. M.; et al. *Atmos. Chem. Phys.* **2011**, *11*, 10219.

(11) Chen, Q.; Liu, Y.; Donahue, N. M.; Shilling, J. E.; Martin, S. T. *Environ. Sci. Technol.* **2011**, *45*, 4763.

(12) Bouvier-Brown, N. C.; Goldstein, A. H.; Gilman, J. B.; Kuster, W. C.; de Gouw, J. A. *Atmos. Chem. Phys.* **2009**, *9*, 5505.

(13) Ravishankara, A. R. *Science* **1997**, *276*, 1058.

(14) Poschl, U. R., Y.; Ammann, M. *Atmos. Chem. Phys.* **2007**, *7*, 5989.

(15) Tolbert, M. A.; Rossi, M. J.; Malhotra, R.; Golden, D. M. *Science* **1987**, *238*, 1258.

(16) Fairbrother, H.; Geiger, F. M.; Grassian, V.; Hemminger, J. C. *J. Phys. Chem. C* **2009**, *113*, 2035.

(17) Jungwirth, P.; Finlayson-Pitts, B. J.; Tobias, D. J. *Chem. Rev.* **2006**, *106*, 1137.

(18) Finlayson-Pitts, B. J. *Chem. Rev.* **2003**, *103*, 4801.

(19) Zondlo, M. A.; Hudson, P. K.; Prenni, A. J.; Tolbert, M. A. *Annu. Rev. Phys. Chem.* **2000**, *51*, 473.

(20) Rudich, Y. *Chem. Rev.* **2003**, *103*, 5097.

(21) Prather, K. A.; Hatch, C. D.; Grassian, V. H. *Annu. Rev. Anal. Chem.* **2008**, *1*, 485.

(22) Usher, C. R.; Michel, A. E.; Grassian, V. H. *Chem. Rev.* **2003**, *103*, 4883.

(23) Martin, S. T. *Chem. Rev.* **2000**, *100*, 3403.

(24) Richmond, G. L. *Chem. Rev.* **2002**, *102*, 2693.

(25) D'Andrea, T. M. D.; Zhang, X.; Jochnowitz, E. B.; Lindeman, T. G.; Simpson, C. J. S. M.; David, D. E.; Curtiss, T. J.; Morris, J. R.; Ellison, G. B. *J. Phys. Chem. B* **2008**, *112*, 535.

(26) Gopalakrishnan, S.; Liu, D.; Allen, H. C.; Kuo, M.; Shultz, M. J. *Chem. Rev.* **2006**, *106*, 1155.

(27) Ghosal, S.; Hemminger, J. C.; Bluhm, H.; Mun, B. S.; Hebenstreit, E. L. D.; Ketteler, G.; Ogletree, D. F.; Requejo, F. G.; M., S. *Science* **2005**, *307*, 563.
(28) Knipping, E. M.; Lakin, M. J.; Foster, K. L.; Jungwirth, P.; Tobias, D. J.; Gerber, R. B.; Dabdub, D.; Finlayson-Pitts, B. J. *Science* **2000**, *288*, 301.
(29) Davidovits, P.; Kolb, C. E.; Williams, L. R.; Jayne, J. T.; Worsnop, D. R. *Chem. Rev.* **2006**, *106*, 1323.
(30) Molina, M. J. *CHEMRAWN VII: Chemistry of the Atmosphere: The Impact of Global Change*; Blackwell Science Publishers: New York, 1994.
(31) Roberts, J. T. *Acc. Chem. Res.* **1998**, *31*, 415.
(32) Tabazadeh, A.; Turco, R. P. *J. Geophys. Res., [Atmos.]* **1993**, *98*, 12727.
(33) King, M. D.; Thompson, K. C.; Ward, A. D. *J. Am. Chem. Soc.* **2004**, *126*, 16710.
(34) Hallquist, M.; Wenger, J. C.; Baltensperger, U.; Rudich, Y.; Simpson, D.; Claeys, M.; Dommen, J.; Donahue, N. M.; George, C.; Goldstein, A. H.; et al. *Adv. Chem. Phys.* **2009**, *9*, 5155.
(35) Goldstein, A. H.; Galbally, I. E. *Environ. Sci. Technol.* **2007**, *41*, 1515.
(36) Kanakidou, M.; Seinfeld, J. H.; Pandis, S. N.; Barnes, I.; Dentener, F. J.; Facchini, M. C.; Van Dingenen, R.; Ervens, B.; Nenes, A.; Nielsen, C. J.; et al. *Adv. Chem. Phys.* **2005**, *5*, 1053.
(37) Galbally, I. E.; Lawson, S. J.; Weeks, I. A.; Bentley, S. T.; Gillett, R. W.; Meyer, M.; Goldstein, A. H. *Environ. Chem.* **2007**, *4*, 178.
(38) Donahue, N. M.; Tischuk, J. E.; Marquis, B. J.; Hartz, K. E. H. *Phys. Chem. Chem. Phys.* **2007**, *9*, 2991.
(39) Iinuma, Y.; Boge, O.; Keywood, M.; Gnauk, T.; Herrmann, H. *Environ. Sci. Technol.* **2009**, *43*, 280.
(40) Pun, B. K.; Seigneur, C.; Lohman, K. *Environ. Sci. Technol.* **2006**, *40*, 4722.
(41) Song, C.; Na, K.; Warren, B.; Malloy, Q.; Cocker, D. R. *Environ. Sci. Technol.* **2007**, *41*, 6990.
(42) Ziemann, P. J. *J. Phys. Chem. A* **2003**, *107*, 2048.
(43) Fenske, J. D.; Kuwata, K. T.; Houk, K. N.; Paulson, S. E. *J. Phys. Chem. A* **2000**, *104*, 7246.
(44) Atkinson, R.; Arey, J. *Acc. Chem. Res.* **1998**, *31*, 574.
(45) Kalberer, M.; Paulsen, D.; Sax, M.; Steinbacher, M.; Dommen, J.; Prevot, A. S. H.; Fisseha, R.; Weingartner, E.; Frankevich, V.; Zenobi, R.; Baltensperger, U. *Science* **2004**, *303*, 1659.
(46) Mueller, L.; Reinnig, M.-C.; Warnke, J.; Hoffmann, T. *Adv. Chem. Phys.* **2008**, *8*, 1423.
(47) Gao, Y.; Hall, W. A.; Johnston, M. V. *Environ. Sci. Technol.* **2010**, *44*, 7897.
(48) Yasmeen, F.; Vermeylen, R.; Szmigielski, R.; Linuma, Y.; Boege, O.; Herrmann, H.; Maenhaut, W.; Claeys, M. *Adv. Chem. Phys.* **2010**, *10*, 10865.
(49) Claeys, M.; Iinuma, Y.; Szmigielski, R.; Surratt, J. D.; Blockhuys, F.; Van Alsenoy, C.; Boege, O.; Sierau, B.; Gomez-Gonzalez, Y.; Vermeylen, R.; et al. *Environ. Sci. Technol.* **2009**, *43*, 6976.
(50) Paulot, F.; Crounse, J. D.; Kjaergaard, H. G.; Kurten, A.; St Clair, J. M.; Seinfeld, J. H.; Wennberg, P. O. *Science* **2009**, *325*, 730.
(51) Crounse, J. D.; Paulot, F.; Kjaergaard, H. G.; Wennberg, P. O. *Phys. Chem. Chem. Phys.* **2011**, *13*, 13607.
(52) Tolocka, M. P.; Jang, M.; Ginter, J. M.; Xoc, F. J.; Kamens, R. M.; Johnston, M. V. *Environ. Sci. Technol.* **2004**, *38*, 1428.
(53) Kroll, J. H.; Seinfeld, J. H. *Atmos. Environ.* **2008**, *42*, 3593.
(54) Docherty, K. S.; Wu, W.; Kim, Y. B.; Ziemann, P. J. *Environ. Sci. Technol.* **2005**, *39*, 4049.
(55) Heaton, K. J.; Sleighter, R. L.; Hatcher, P. G.; Hall, W. A., IV; Johnston, M. V. *Environ. Sci. Technol.* **2009**, *43*, 7797.
(56) Hari, P.; Kulmala, M. *Boreal Environ. Res.* **2005**, *10*, 315.
(57) Andreae, M. O.; Artaxo, P.; Brandao, C.; Carswell, F. E.; Ciccioli, P.; da Costa, A. L.; Culf, A. D.; Esteves, J. L.; Gash, J. H. C.; Grace, J.; et al. *J. Geophys. Res.* **2002**, *107*, 8066.
(58) Guenther, A.; Hewitt, C. N.; Erickson, D.; Fall, R.; Geron, C.; Graedel, T.; Harley, P.; Klinger, L.; Lerdau, M.; McKay, W. A.; et al. *J. Geophys. Res., [Atmos.]* **1995**, *100*, 8873.
(59) Kesselmeier, J.; Guenther, A.; Hoffmann, T.; Warnke, J. In *Amazonia and Global Change*; Keller, M., Bustamante, M., Gash, J., Silva Dias, P. S., Eds.; 2009; Vol. 186, p 183.
(60) Vrekoussis, M.; Wittrock, F.; Richter, A.; Burrows, J. P. *Atmos. Chem. Phys.* **2009**, *13*, 4485.
(61) Lelieveld, J.; Butler, T. M.; Crowley, J. N.; Dillon, T. J.; Fischer, H.; Ganzeveld, L.; Harder, H.; Lawrence, M. G.; Martinez, M.; Taraborrelli, D.; Williams, J. *Nature* **2008**, *452*, 737.
(62) Artaxo, P.; Maenhaut, W.; Storms, H.; Vangrieken, R. *J. Geophys. Res., [Atmos.]* **1990**, *95*, 16971.
(63) Andreae, M. O. *Science* **2007**, *315*, 50.
(64) Andreae, M. O.; Artaxo, P.; Brandao, C.; Carswell, F. E.; Ciccioli, P.; da Costa, A. L.; Culf, A. D.; Esteves, J. L.; Gash, J. H. C.; Grace, J.; et al. *J. Geophys. Res., [Atmos.]* **2002**, *107*, 8066.
(65) Claeys, M.; Graham, B.; Vas, G.; Wang, W.; Vermeylen, R.; Pashynska, V.; Cafmeyer, J.; Guyon, P.; Andreae, M. O.; Artaxo, P.; Maenhaut, W. *Science* **2004**, *303*, 1173.
(66) Gerab, F.; Artaxo, P.; Gillett, R.; Ayers, G. *Nucl. Instrum. Methods Phys. Res. B* **1998**, *137*, 955.
(67) Martin, S. T.; Andreae, M. O.; Artaxo, P.; Baumgardner, D.; Chen, Q.; Goldstein, A. H.; Guenther, A.; Heald, C. L.; Mayol-Bracero, O. L.; McMurry, P. H.; et al. *Rev. Geophys.* **2010**, *48*, RG2002.
(68) Poeschl, U.; Martin, S. T.; Sinha, B.; Chen, Q.; Gunthe, S. S.; Huffman, J. A.; Borrmann, S.; Farmer, D. K.; Garland, R. M.; Helas, G.; et al. *Science* **2010**, *329*, 1513.
(69) Goldstein, A. H.; Hultman, N. E.; Fracheboud, J. M.; Bauer, M. R.; Panek, J. A.; Xu, M.; Qi, Y.; Guenther, A. B.; Baugh, W. *Agric. For. Meteorol.* **2000**, *101*, 113.
(70) Murphy, J. G.; Day, A.; Cleary, P. A.; Wooldridge, P. J.; Cohen, R. C. *Adv. Chem. Phys.* **2006**, *6*, 5321.
(71) Marple, V. A.; Rubow, K. L.; Behm, S. M. *Aerosol Sci. Technol.* **1991**, *14*, 434.
(72) In *IPCC 2007 Assessment Report 4*; Pachauri, R. K., Reisinger, A., Eds.; IPCC: Geneva, Switzerland, 2007; p 104.
(73) Wang, S. C.; Flagan, R. C. *Aerosol Sci. Technol.* **1990**, *13*, 230.
(74) Ehn, M.; Junninen, H.; Schobesberger, S.; Manninen, H. E.; Franchin, A.; Sipila, M.; Petaja, T.; Kerminen, V. M.; Tammet, H.; Mirme, A.; et al. *Aerosol Sci. Technol.* **2011**, *45*, 522.
(75) Junninen, H.; Ehn, M.; Petaja, T.; Luosujarvi, L.; Kotiaho, T.; Kostiainen, R.; Rohner, U.; Gonin, M.; Fuhrer, K.; Kulmala, M.; Worsnop, D. R. *Atmos. Meas. Technol.* **2010**, *3*, 1039.
(76) Ehn, M.; Junninen, H.; Petaja, T.; Kurten, T.; Kerminen, V. M.; Schobesberger, S.; Manninen, H. E.; Ortega, I. K.; Vehkamaki, H.; Kulmala, M.; Worsnop, D. R. *Atmos. Chem. Phys.* **2010**, *10*, 8513.
(77) Kirkby, J.; Curtius, J.; Almeida, J.; Dunne, E.; Duplissy, J.; Ehrhart, S.; Franchin, A.; Gagne, S.; Ickes, L.; Kuerten, A.; et al. *Nature* **2011**, *476*, 429.
(78) Petaja, T.; Mauldin, R. L., III; Kosciuch, E.; McGrath, J.; Nieminen, T.; Paasonen, P.; Boy, M.; Adamov, A.; Kotiaho, T.; Kulmala, M. *Atmos. Chem. Phys.* **2009**, *9*, 7435.
(79) Jokinen, T.; Sipilä, M.; Junninen, H.; Ehn, M.; Lönn, G.; Hakala, J.; Petäjä, T.; Mauldin, R. L., III; Kulmala, M.; Worsnop, D. R. *Atmos. Chem. Phys. Discuss* **2011**, *11*, 31983.
(80) Kulmala, M.; Riipinen, I.; Sipila, M.; Manninen, H. E.; Petaja, T.; Junninen, H.; Dal Maso, M.; Mordas, G.; Mirme, A.; Vana, M.; et al. *Science* **2007**, *318*, 89.
(81) Sipila, M; Berndt, T.; Petaja, T.; Brus, D.; Vanhanen, J.; Stratmann, F.; Patokoski, J.; Mauldin, R. L., III; Hyvarinen, A.-P.; Lihavainen, H.; Kulmala, M. *Science* **2010**, *327*, 1243.
(82) Suess, D. T.; Prather, K. A. *Chem. Rev.* **1999**, *99*, 3007.
(83) Noble, C. A.; Prather, K. A. *Mass Spectrom. Rev.* **2000**, *19*, 248.
(84) Walser, M. L.; Desyaterik, Y.; Laskin, J.; Laskin, A.; Nizkorodov, S. A. *Phys. Chem. Chem. Phys.* **2008**, *10*, 1009.
(85) Walser, M. L.; Park, J.; Gomez, A. L.; Russell, A. R.; Nizkorodov, S. A. *J. Phys. Chem. A* **2007**, *111*, 1907.
(86) Jayne, J. T.; Leard, D. C.; Zhang, X.; Davidovits, P.; Smith, K. A.; Kolb, C. E.; Worsnop, D. R. *Aerosol Sci. Technol.* **2000**, *33*, 49−70.

(87) DeCarlo, P. F.; Kimmel, J. R.; Trimborn, A.; Northway, M. J.; Jayne, J. T.; Aiken, A. C.; Gonin, M.; Fuhrer, K.; Horvath, T.; Docherty, K. S.; et al. *Anal. Chem.* **2006**, *78*, 8281.
(88) Jimenez, J. L.; Canagaratna, M. R.; Donahue, N. M.; Prevot, A. S. H.; Zhang, Q.; Kroll, J. H.; DeCarlo, P. F.; Allan, J. D.; Coe, H.; Ng, N. L.; et al. *Science* **2009**, *326*, 1525.
(89) Heaton, K. J.; Dreyfus, M. A.; Wang, S.; Johnston, M. V. *Environ. Sci. Technol.* **2007**, *41*, 6129.
(90) Heaton, K. J.; Sleighter, R. L.; Hatcher, P. G.; Hall Iv, W. A.; Johnston, M. V. *Environ. Sci. Technol.* **2009**, *43*, 7797.
(91) Aiken, A. C.; Decarlo, P. F.; Kroll, J. H.; Worsnop, D. R.; Huffman, J. A.; Docherty, K. S.; Ulbrich, I. M.; Mohr, C.; Kimmel, J. R.; Sueper, D.; et al. *Environ. Sci. Technol.* **2008**, *42*, 4478.
(92) Ebben, C. J.; Martinez, I. S.; Shrestha, M.; Buchbinder, A.; Corrigan, A. L.; Guenther, A.; Karl, T.; Petaejae, T.; Song, W. W.; Zorn, S. R.; et al. *Atmos. Chem. Phys.* **2011**, *11*, 10317.
(93) Frosch, M.; Bilde, M.; DeCarlo, P. F.; Juranyi, Z.; Tritscher, T.; Dommen, J.; Donahue, N. M.; Gysel, M.; Weingartner, E.; Baltensperger, U. *J. Geophys. Res., [Atmos.]* **2011**, 116.
(94) King, S. M.; Rosenoern, T.; Shilling, J. E.; Chen, Q.; Martin, S. T. *Geophys. Res. Lett.* **2007**, *34*.
(95) Kuwata, M.; Chen, Q.; Martin, S. T. *Phys. Chem. Chem. Phys.* **2011**, *13*, 14571.
(96) Lee, B. H.; Pierce, J. R.; Engelhart, G. J.; Pandis, S. N. *Atmos. Environ.* **2011**, *45*, 2443.
(97) Shilling, J. E.; Chen, Q.; King, S. M.; Rosenoern, T.; Kroll, J. H.; Worsnop, D. R.; DeCarlo, P. F.; Aiken, A. C.; Sueper, D.; Jimenez, J. L.; Martin, S. T. *Atmos. Chem. Phys.* **2009**, *9*, 771.
(98) Shilling, J. E.; Chen, Q.; King, S. M.; Rosenoern, T.; Kroll, J. H.; Worsnop, D. R.; McKinney, K. A.; Martin, S. T. *Atmos. Chem. Phys.* **2008**, *8*, 2073.
(99) Stanier, C. O.; Pathak, R. K.; Pandis, S. N. *Environ. Sci. Technol.* **2007**, *41*, 2756.
(100) Wang, J.; Doussin, J. F.; Perrier, S.; Perraudin, E.; Katrib, Y.; Pangui, E.; Picquet-Varrault, B. *Atmos. Meas. Technol.* **2011**, *4*, 2465.
(101) Kiendler-Scharr, A.; Wildt, J.; Dal Maso, M.; Hohaus, T.; Kleist, E.; Mentel, T. F.; Tillmann, R.; Uerlings, R.; Schurr, U.; Wahner, A. *Nature* **2009**, *461*, 381.
(102) Tritscher, T.; Dommen, J.; DeCarlo, P. F.; Gysel, M.; Barmet, P. B.; Praplan, A. P.; Weingartner, E.; Prevot, A. S. H.; Riipinen, I.; Donahue, N. M.; Baltensperger, U. *Atmos. Chem. Phys.* **2011**, *11*, 11477.
(103) George, I. J.; Abbatt, J. P. D. *Atmos. Chem. Phys.* **2010**, *10*, 5551.
(104) Nojgaard, J. K.; Norgaard, A. W.; Wolkoff, P. *Atmos. Environ.* **2007**, *41*, 8345.
(105) Rohr, A. C.; Weschler, C. J.; Koutrakis, P.; Spengler, J. D. *Aerosol Sci. Technol.* **2003**, *37*, 65.
(106) Tolocka, M. P.; Heaton, K. J.; Dreyfus, M. A.; Wang, S. Y.; Zordan, C. A.; Saul, T. D.; Johnston, M. V. *Environ. Sci. Technol.* **2006**, *40*, 1843.
(107) Gao, Y. Q.; Hall, W. A.; Johnston, M. V. *Environ. Sci. Technol.* **2010**, *44*, 7897.
(108) Docherty, K. S.; Wu, W.; Lim, Y. B.; Ziemann, P. J. *Environ. Sci. Technol.* **2005**, *39*, 4049.
(109) Tobias, H. J.; Ziemann, P. J. *Anal. Chem.* **1999**, *71*, 3428.
(110) Chow, J. C.; Yu, J. Z.; Watson, J. G.; Ho, S. S. H.; Bohannan, T. L.; Hays, M. D.; Fung, K. K. *J. Environ. Sci. Health Part A: Toxic/Hazard. Subst. Environ. Eng.* **2007**, *42*, 1521.
(111) Bateman, A. P.; Nizkorodov, S. A.; Laskin, J.; Laskin, A. *Phys. Chem. Chem. Phys.* **2009**, *11*, 7931.
(112) Bateman, A. P.; Walser, M. L.; Desyaterik, Y.; Laskin, J.; Laskin, A.; Nizkorodov, S. A. *Environ. Sci. Technol.* **2008**, *42*, 7341.
(113) Laskin, J.; Laskin, A.; Roach, P. J.; Slysz, G. W.; Anderson, G. A.; Nizkorodov, S. A.; Bones, D. L.; Nguyen, L. Q. *Anal. Chem.* **2010**, *82*, 2048.
(114) Schwier, A. N.; Sareen, N.; Mitroo, D.; Shapiro, E. L.; McNeill, V. F. *Environ. Sci. Technol.* **2010**, *44*, 6174.
(115) Duarte, R.; Duarte, A. C. *TrAC-Trends Anal. Chem.* **2011**, *30*, 1659.
(116) Takahama, S.; Liu, S.; Russell, L. M. *J. Geophys. Res., [Atmos.]* **2010**, *115*.
(117) Russell, L. M.; Bahadur, R.; Ziemann, P. J. *Proc. Natl. Acad. Sci. U. S. A.* **2011**, *108*, 3516.
(118) Prenni, A. J.; Petters, M. D.; Kreidenweis, S. M.; Heald, C. L.; Martin, S. T.; Artaxo, P.; Garland, R. M.; Wollny, A. G.; Poschl, U. *Nat. Geosci.* **2009**, *2*, 401.
(119) Poeschl, U.; Martin, S. T.; Sinha, B.; Chen, Q.; Gunthe, S. S.; Huffman, J. A.; Borrmann, S.; Farmer, D. K.; Garland, R. M.; Helas, G.; et al. *Science* **2010**, *329*, 1513.
(120) Bertram, A. K.; Martin, S. T.; Hanna, S. J.; Smith, M. L.; Bodswortgh, A.; Q., C.; M., K.; Liu, A.; Zorn, S. R. *Atmos. Chem. Phys.* **2011**.
(121) Liu, S.; Takahama, S.; Russell, L. M.; Gilardoni, S.; Baumgardner, D. *Atmos. Chem. Phys.* **2009**, *9*, 6849.
(122) McMurry, P. H. *Atmos. Environ.* **2000**, *34*, 1959.
(123) Virtanen, A.; Joutsensaari, J.; Koop, T.; Kannosto, J.; Yli-Pirila, P.; Leskinen, J.; Makela, J. M.; Holopainen, J. K.; Poschl, U.; Kulmala, M.; Worsnop, D. R.; Laaksonen, A. *Nature* **2010**, *467*, 824.
(124) Takahama, S.; Gilardoni, S.; Russell, L. M.; Kilcoyne, A. L. D. *Atmos. Environ.* **2007**, *41*, 9435.
(125) Holmes, N. S. *Atmos. Environ.* **2007**, *41*, 2183.
(126) Zhu, X. D.; Suhr, H. J.; Shen, Y. R. *J. Opt. Soc. Am. B* **1986**, *3*, P252.
(127) Shen, Y. R. *The Principles of Nonlinear Optics*; John Wiley & Sons: New York, 1984.
(128) Watry, M. R.; Brown, M. G.; Richmond, G. L. *Appl. Spectrosc.* **2001**, *55*, 321A.
(129) Esenturk, O.; Walker, R. A. *J. Phys. Chem. B.* **2004**, *108*, 10631.
(130) Eisenthal, K. B. *Chem. Rev.* **1996**, *96*, 1343.
(131) Buck, M.; Himmelhaus, M. *J. Vac. Sci. Technol. A* **2001**, *19*, 2717.
(132) Geiger, F. M. *Annu. Rev. Phys. Chem.* **2009**, *60*, 61.
(133) Konek, C. T.; Musorrafiti, M. J.; Al-Abadleh, H. A.; Bertin, P. A.; Nguyen, S. T.; Geiger, F. M. *J. Am. Chem. Soc.* **2004**, *126*, 11754.
(134) Voges, A. B.; Al-Abadleh, H. A.; Geiger, F. M. In *Environmental Catalysis*; Grassian, V. H., Ed.; CRC Press: Boca Raton, FL, 2005.
(135) Voges, A. B.; Stokes, G. Y.; Gibbs-Davis, J. M.; Lettan, R. B.; Bertin, P. A.; Pike, R. C.; Nguyen, S. T.; Scheidt, K. A.; Geiger, F. M. *J. Phys. Chem. C* **2007**, *111*, 1567.
(136) Stokes, G. Y.; Buchbinder, A. M.; Gibbs-Davis, J. M.; Scheidt, K. A.; Geiger, F. M. *Vibr. Spectrosc.* **2009**, *50*, 86.
(137) Stokes, G. Y.; Chen, E. H.; Buchbinder, A. M.; Paxton, W. F.; Keeley, A.; Geiger, F. M. *J. Am. Chem. Soc.* **2009**, *131*, 13733.
(138) Stokes, G. Y.; Chen, E. H.; Walter, S. R.; Geiger, F. M. *J. Phys. Chem. A* **2009**, *113*, 8985.
(139) Richmond, G. L. *Annu. Rev. Phys. Chem.* **2001**, *52*, 357.
(140) Scatena, L. F.; Brown, M. G.; Richmond, G. L. *Science* **2001**, *292*, 908.
(141) Shen, Y. R.; Ostroverkhov, V. *Chem. Rev.* **2006**, *106*, 1140.
(142) Liu, D. F.; Ma, G.; Levering, L. M.; Allen, H. C. *J. Phys. Chem. B* **2004**, *108*, 2252.
(143) Mucha, M.; Frigato, T.; Levering, L. M.; Allen, H. C.; Tobias, D. J.; Dang, L. X.; Jungwirth, P. *J. Phys. Chem. B* **2005**, *109*, 7617.
(144) Voss, L. F.; Bazerbashi, M. F.; Beekman, C. P.; Hadad, C. M.; Allen, H. C. *J. Geophys. Res.* **2007**, *112*, D06209.
(145) Allen, H. C.; Gragson, D. E.; Richmond, G. L. *J. Phys. Chem. B* **1999**, *103*, 660.
(146) Tarbuck, T. L.; Richmond, G. L. *J. Am. Chem. Soc.* **2006**, *128*, 3256.
(147) Shen, Y. R. *The Principles of Nonlinear Optics*; John Wiley & Sons, Inc.: Hoboken, NJ, 2003.
(148) Walter, S. R.; Geiger, F. M. *J. Phys. Chem. Lett.* **2009**, *1*, 9.
(149) Buchbinder, A. M.; Ray, N. A.; Lu, J.; Van Duyne, R. P.; Stair, P. C.; Weitz, E.; Geiger, F. M. *J. Am. Chem. Soc.* **2011**, *133*, 17816.
(150) Achtyl, J. L.; Buchbinder, A. M.; Geiger, F. M. *J. Phys. Chem. Lett.* **2012**, *3*, 280.
(151) Konek, C. T.; Illg, K. D.; Al-Abadleh, H. A.; Voges, A. B.; Yin, G.; Musorrafiti, M. J.; Schmidt, C. M.; Geiger, F. M. *J. Am. Chem. Soc.* **2005**, *127*, 15771.

(152) Boman, F. C.; Gibbs-Davis, J. M.; Heckman, L. M.; Stepp, B. R.; Nguyen, S. T.; Geiger, F. M. *J. Am. Chem. Soc.* **2009**, *131*, 844.
(153) Wang, H.; Yan, E. C. Y.; Borguet, E.; Eisenthal, K. B. *Chem. Phys. Lett.* **1996**, *259*, 15.
(154) Eisenthal, K. B. *Chem. Rev.* **2006**, *106*, 1462.
(155) Ma, G.; Allen, H. C. *J. Am. Chem. Soc.* **2002**, *124*, 9374.
(156) de Beer, A. G. F.; Roke, S. *Phys. Rev. B* **2007**, *75*, 245438.
(157) Dadap, J. I.; de Aguiar, H. B.; Roke, S. *J. Chem. Phys.* **2009**, *130*, 214710.
(158) Wang, H.; Troxler, T.; Yeh, A.-G.; Dai, H.-L. *Langmuir* **2000**, *16*, 2475.
(159) Ebben, C. J.; Zorn, S. R.; Lee, S.-B.; Artaxo, P.; Martin, S. T.; Geiger, F. M. *Geophys. Res. Lett.* **2011**, *38*, L16807.
(160) Martinez, I. S.; Peterson, M. D.; Ebben, C. J.; Hayes, P. L.; Artaxo, P.; Martin, S. T.; Geiger, F. M. *Phys. Chem. Chem. Phys.* **2011**, *13*, 12114.
(161) Hayes, P. L.; Chen, E. H.; Achtyl, J. L.; Geiger, F. M. *J. Phys. Chem. A* **2009**, *113*, 4269.
(162) Voges, A. B.; Al-Abadleh, H. A.; Geiger, F. M. In *Environmental Catalysis*; Grassian, V., Ed.; CRC Press: Boca Raton, FL, 2005.
(163) Esenturk, O.; Walker, R. A. *J. Phys. Chem. B* **2004**, *108*, 10631.
(164) *Handbook of Chemistry and Physics: A Ready-Reference Book of Chemical and Physical Data*; 78 ed.; CRC Press, Inc.: Boca Raton, FL, 1997.
(165) Buchbinder, A. M.; Weitz, E.; Geiger, F. M. *J. Phys. Chem. C* **2010**, *114*, 554.
(166) Chen, C. Y.; Even, M. A.; Wang, J.; Chen, Z. *Macromolecules* **2002**, *35*, 9130.
(167) Opdahl, A.; Phillips, R. A.; Somorjai, G. A. *J. Phys. Chem. B* **2002**, *106*, 5212.
(168) Miranda, P. B.; Shen, Y. R. *J. Phys. Chem. B* **1999**, *103*, 3292.
(169) Ehn, M.; Kleist, E.; Junninen, H.; Petäjä, T.; Lönn, G.; Schobesberger, S.; Dal Maso, M.; Trimborn, A.; Kulmala, M.; Worsnop, D. R.; Wahner, A.; Wildt, J.; Mentel, T. F. *Atmos. Chem. Phys. Discuss* **2012**, *12*, 4589.
(170) Barnette, A. L.; Bradley, L. C.; Veres, B. D.; Schreiner, E. P.; Park, Y. B.; Park, J.; Park, S.; Kim, S. H. *Biomacromolecules* **2011**, *12*, 2434.
(171) Takahama, S.; Schwartz, R. E.; Russell, L. M.; Macdonald, A. M.; Sharma, S.; Leaitch, W. R. *Atmos. Chem. Phys.* **2011**, *11*, 6367.
(172) Dal Maso, M.; Kulmala, M.; Riipinen, I.; Wagner, R.; Hussein, T.; Aalto, P. P.; Lehtinen, K. E. J. *Boreal Environ. Res.* **2005**, *10*, 323.
(173) Stokes, G. Y.; Chen, E. H.; Buchbinder, A. M.; Geiger, F. M. *J. Am. Chem. Soc.* **2009**, *131*, 13733.
(174) Phillips, M. A.; Wildung, M. R.; Williams, D. C.; Hyatt, D. C.; Croteau, R. *Arch. Biochem. Biophys.* **2003**, *411*, 267.
(175) Ellison, G. B.; Tuck, A. F.; Vaida, V. *J. Geophys. Res.* **1999**, *104*, 11633.
(176) Oberbeck, V. R.; Marshall, J.; Shen, T. *J. Molec. Evol.* **1991**, *32*, 296.
(177) Colombo, L. M.; Thomas, R. M.; Luisi, P. L. *Chirality* **1991**, *3*, 233.
(178) Yassaa, N.; Williams, J. *Atmos. Environ.* **2005**, *39*, 4875.
(179) Williams, J.; Yassaa, N.; Bartenbach, S.; Lelieveld, J. *Adv. Chem. Phys.* **2007**, *7*, 973.
(180) Armstrong, D. W.; Kullman, J. P.; Chen, X. H.; Rowe, M. *Chirality* **2001**, *13*, 153.
(181) Salma, I.; Meszaros, T.; Maenhaut, W.; Vass, E.; Majer, Z. *Atmos. Chem. Phys.* **2010**, *10*, 1315.
(182) Noziere, B.; Gonzalez, N. J. D.; Borg-Karlson, A.-K.; Pei, Y.; Redeby, J. P.; Krejci, R.; Dommen, J.; Prevot, A. S. H.; Anthonsen, T. *Geophys. Res. Lett.* **2011**, *38*.
(183) Song, W.; Williams, J.; Yassaa, N.; Martinez, M.; Carnero, J. A. A.; Hildalgo, P. J.; Bozem, H.; Lelieveld, J. *J. Atmos. Chem.* **2011**, *68*, 233.
(184) Boyd, R. W. *Nonlinear Optics*; Academic Press: New York, 2003.
(185) Eerdekens, G.; Yassaa, N.; Sinha, V.; Aalto, P. P.; Aufmhoff, H.; Arnold, F.; Fiedler, V.; Kulmala, M.; Williams, J. *Atmos. Chem. Phys.* **2009**, *9*, 8331.
(186) Eerdekens, G.; Yaassaa, N.; Sinha, V.; Aalto, P. P.; Aufmhoff, H.; Arnold, F.; Fiedler, V.; Kulmala, M.; Williams, J. *Adv Chem. Phys.* **2009**, *9*, 8331.
(187) Liao, L.; Dal Maso, M.; Taipale, R.; Rinne, J.; Ehn, M.; Junninen, H.; Aeijaelae, M.; Nieminen, T.; Alekseychik, P.; Hulkkonen, M.; et al. *Boreal Environ. Res.* **2011**, *16*, 288.
(188) Tarraborrelli, D.; Lawrence, M. G.; Crowley, J. N.; Dillon, T. J.; Gromov, S.; Gross, C. B.; Vereecken, L.; Lelieveld, J. *Nat. Geosci.* **2012**, *5*, 190.
(189) Paulot, F.; Crounse, J. D.; Kjaergaard, H. G.; Kurten, A.; St. Clair, J. M.; Seinfeld, J. H.; Wennberg, P. O. *Science* **2009**, *325*, 730.
(190) Claeys, M.; Graham, B.; Vas, G.; Vermeylen, R.; Pashynska, V.; Cafmeyer, J.; Guyon, P.; Andreae, M. O.; Artaxo, P.; Maenhunt, W. *Science* **2004**, *303*, 1173.
(191) Peterson, M. D.; Hayes, P. L.; Martinez, I. S.; Cass, L. C.; Achtyl, J. A.; Weiss, E. A.; Geiger, F. M. *Opt. Mater. Exp.* **2011**, *1*, 57.
(192) Jacobson, M. Z. *Geophys. Res. Lett.* **2000**, *27*, 217.
(193) Odum, J. R.; Jungkamp, T. P. W.; Griffin, R. J.; Flagan, R. C.; Seinfeld, J. H. *Science* **1997**, *276*, 96.
(194) Achtyl, J. A.; Buchbinder, A. M.; Geiger, F. M. *J. Phys. Chem. Lett.* **2012**, *3*, 280.
(195) Kim, H. D.; Balgar, T.; Hasselbrink, E. *Chem. Phys. Lett.* **2011**, *508*, 1.
(196) Andrews, A. B.; McClelland, A.; Korkeila, O.; Demidov, A.; Krummel, A.; Mullins, O. C.; Chen, Z. *Langmuir* **2011**, *27*, 6049.
(197) Baeck, J.; Aalto, J.; Henrikson, M.; Hakola, H.; He, Q.; Boy, M. *Biogeosciences* **2012**, *9*, 689.
(198) Sugiharto, A. B.; Johnson, C. M.; Dunlop, I. E.; Roke, S. *J. Phys. Chem. C* **2008**, *112*, 7531.
(199) Jubb, A. M.; Allen, H. C. *J. Phys. Chem. C* **2012**, *116*, 9085.
(200) Chen, X.; Allen, H. C. *J. Phys. Chem. A* **2009**, *113*, 12655.
(201) Fu, L.; Liu, J.; Yan, E. C. Y. *J. Am. Chem. Soc.* **2011**, *133*, 8094.
(202) Pöschl, U.; Rudich, Y.; Ammann, M. *Atmos. Chem. Phys.* **2007**, *7*, 5989.
(203) Karl, T.; Guenther, A.; Yokelson, R. J.; Greenberg, J. P.; Potosnak, M.; Blake, D. R.; Artaxo, P. *J. Geophys. Res.* **2007**, *112*, D18302.
(204) Lelieveld, J.; Butler, T. M.; Crowley, J. N.; Dillon, T. J.; Fischer, H.; Ganzeveld, L.; Harder, H.; Lawrence, M. G.; Martinez, M.; Taraborrelli, D.; Williams, J. *Nature* **2008**, *452*, 737.